Acta Zoologica (Stockholm) **88**: 000–000 (April 2007) doi: 10.1111/j.1463-6395.2007.00318.x

Anatomy and systematics of the minute syrnolopsine gastropods from Lake Tanganyika (Caenogastropoda, Cerithioidea, Paludomidae)

Ellen E. Strong[1] and Matthias Glaubrecht[2]

[1]Smithsonian Institution, National Museum of Natural History, PO Box 37012, MRC 163, Washington, D.C. 20013-7012, USA; [2]Department of Malacozoology, Museum of Natural History Berlin, Humboldt University, Invalidenstrasse 43, D-10115 Berlin, Germany

Keywords:
Freshwater, homology, phylogeny, size reduction

Accepted for publication:
25 October 2007

Abstract

Strong, E. E. and Glaubrecht, M. 2007. Anatomy and systematics of the minute syrnolopsine gastropods from Lake Tanganyika (Caenogastropoda, Cerithioidea, Paludomidae). — *Acta Zoologica* (Stockholm) **88**: 000–000

The minute syrnolopsine gastropods endemic to Lake Tanganyika have been allied to a number of freshwater, marine and terrestrial groups as a consequence of superficial conchological similarity. Although early anatomical studies confirmed the cerithioid organization of this clade, their close relationship to other lake species was not consistently recognized. In several recent cladistic analyses based on molecular data, the higher taxonomic placement and sister group relationships of syrnolopsines have been unstable. The present analysis confirms that syrnolopsines possess a spermatophore-forming organ – a synapomorphy of the Paludomidae – corroborating their placement in this family. Consistent with the molecular data, syrnolopsine monophyly is supported by two characters that occur exclusively in this group (salivary gland ducts that bypass the nerve ring and a linear albumen gland). Several characters in *Martelia tanganyicensis* – the most diminutive syrnolopsine – are only evident in the smallest lake species thus far investigated (*Bridouxia*, *Stormsia*) namely reduction of ctenidial leaflets, sorting area, intestine length and number of statoconia. These features are interpreted as being correlated with reduction in size. Nevertheless, close examination reveals differences in detail that allow more refined hypotheses of homology and are consistent with their independent origin.

Ellen E. Strong, Smithsonian Institution, National Museum of Natural History, PO Box 37012, MRC 163, Washington, D.C. 20013-7012, U.S.A. E-mail: StrongE@si.edu.

Introduction

Convergence in shell form, particularly of the adult shell, is a widespread and well-documented phenomenon in the gastropods, from within genera to between orders and other higher taxonomic groupings. In particular, ancient lakes are well known for producing gastropod faunas with remarkable conchological similarity to marine forms and/or distantly related non-lacustrine species (see e.g. Gorthner and Meier-Brook 1985; Martens 1997; Van Damme and Pickford 2003). However, Lake Tanganyika stands alone in the spectacular diversity of shell forms it has produced among the endemic thalassoid (i.e. marine-like) cerithioid gastropods and their pervasive conchological convergence with widely divergent families of marine gastropods. This superficial similarity provided the basis for early speculation on the marine origins of this species flock (e.g. Moore 1899, 1903), and more recently has been attributed to coevolutionary predator–prey interactions in conjunction with the physical, sea-like attributes and the longevity of the lake (e.g. Coulter 1991; West *et al.* 1991; West and Cohen 1994, 1996; van Damme and Pickford 2003). This conchological convergence is also responsible for the confusion that reigned for decades concerning their systematic affinities.

The minute thalassoid species currently placed in the Syrnolopsini Bourguignat, 1890 (see Bouchet and Rocroi

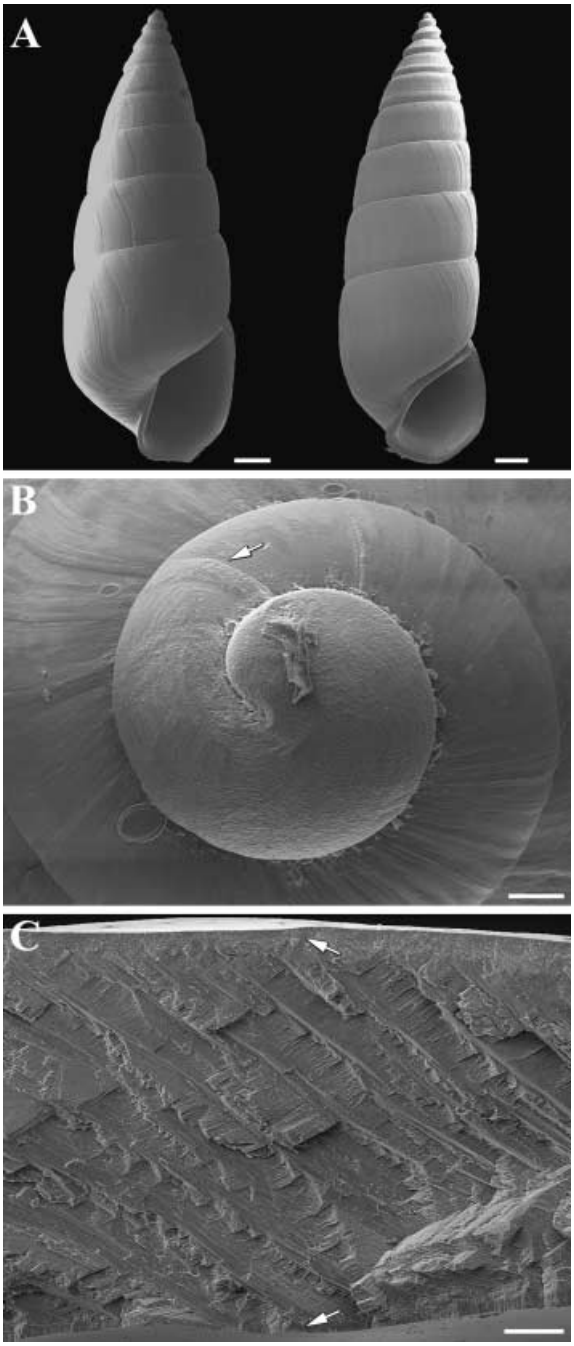

Fig. 1—Shell morphology of *Syrnolopsis lacustris* (ZMB 220078). —**A**. Shell. Apertural view of shells from lot used for anatomical investigations. Note variation in shell width and in development of carina on early whorls. Specimen on left is young adult; specimen on right is adult with thickened aperture. Scale bars, 500 μm. —**B**. Protoconch. Apical view of protoconch with detail of irregular pitted sculpture. Arrow indicates approximate onset of axial growth lines. Scale bar, 30 μm. —**C**. Microstructure. Cross-sectional view, shell exterior is uppermost. Arrows indicate transitions between internal crossed-lamellar layer and outer irregular, prismatic and inner regular, simple prismatic layers. Scale bar, 40 μm.

2005) are characterized by their small, slender shells with a closed umbilicus and a spiral columellar plait (see Fig. 1). These conchological features have resulted in syrnolopsines being allied to the Paludinidae (e.g. Crosse 1881), Rissooidea (e.g. Smith 1881; Pilsbry and Bequaert 1927; Wenz 1939; Bandel 1998), Pyramidellidae (e.g. Ancey 1882; Smith 1890), in or near the Helicidae (e.g. Bourguignat 1885, 1889), and the Hydrobiidae (e.g. Fischer 1887; Thiele 1929). Alternatively, syrnolopsines have been set aside from other thalassoid gastropods in a family of unknown affinity to the remaining lacustrine 'prosobranchs' (e.g. Bourguignat 1890; Germain 1908; Dartevelle and Schwetz 1948) or placed near the Thiaridae (Taylor and Sohl 1962). Indeed, the nominotypical genus earned its name as a consequence of its conchological similarity to the marine pyramidellid *Syrnola* A. Adams, 1860. Syrnolopsines also have the distinction of being among the smallest of the thalassoids inhabiting the lake (see Discussion). Currently, six species are recognized: *Syrnolopsis lacustris* Smith, 1880, *S. minuta* Bourguignat, 1885, *S. gracilis* Pilsbry and Bequaert, 1927, *Anceya giraudi* Bourguignat, 1885, *A. terebriformis* (Smith 1890), and *Martelia tanganyicensis* Dautzenberg, 1908 (see Brown 1994; for nomenclatural details).

Morphological studies by Mandahl-Barth (1954) and Bouillon (1955) confirmed the cerithioid affinities of the Syrnolopsini based on the absence of accessory pedal ganglia and of a copulatory organ, the presence of a smooth mantle edge, a concentrated central nervous system and statocysts with numerous statoconia, as well as a similarity of the radula and operculum to several other cerithioidean taxa in the lake. Insofar that this combination of characters is generally cerithioid (Houbrick 1988), the conclusions of Mandahl-Barth (1954) and Bouillon (1955) were correct. However, today we have a much more thorough understanding of the anatomy and systematics of the Lake Tanganyika thalassoid gastropods, and of freshwater cerithioideans in general.

In this context, the goal of the following account is to satisfy several notable omissions in previous studies, in particular concerning the alimentary and reproductive systems. This new information will be used to confirm their familial placement and explore possible sister group relationships both of which remain unstable in several phylogenetic analyses based on molecular data (West and Michel 2000; Michel 2004; Wilson *et al*. 2004). Additionally, this analysis will examine the features of syrnolopsines in the context of size reduction and the possible consequences for homology assessment.

Materials and Methods

Specimens were examined using a Leica MZ 9.5 binocular microscope with *camera lucida*; visualization of structural details was enhanced through the use of aqueous toluidine blue. Descriptions of midgut morphology are given with the stomach opened dorsally and the style sac uppermost.

Serial histological sections were prepared for one male and one female of each species; tissues were embedded in

paraplast, sectioned at 6 μm, and stained with haematoxylin & eosin–phloxine (Humason 1967).

Typically, two to three specimens were examined for each organ system investigated. However, owing to the small size of the individuals, only one nerve ring was dissected for each species; observations were confirmed with histological sections.

A thorough account is provided for *Syrnolopsis lacustris* – the type species of the type genus for the tribe; only discrete differences are detailed for *Anceya giraudi* and *Martelia tanganyicensis* as compared to the reference taxon, with remarks highlighting more qualitative differences among the species examined. The type locality of *S. lacustris* is indicated only as Lake Tanganyika (Smith 1880); thus, the use of topotypic material was not possible. As adequate information has been published on the shells (Leloup 1953; Mandahl-Barth 1954; Bouillon 1955), the following account will emphasize internal anatomy; although the radulae have been previously described, this represents the first published scanning electron microscopic investigation of syrnolopsine radulae.

Codes for institutions from which material was examined are as follows: MNHN – Muséum national d'Histoire naturelle, Paris; ZMB – Museum für Naturkunde, Humboldt Universität, Berlin (formerly Zoologisches Museum Berlin).

Results

Syrnolopsis lacustris Smith, 1880

Material examined. Zambia: Kasenga Point (08°42.887′S, 31°08.476′E) (ZMB 220005, 220045) (08°42.887′S, 31°08.476′E, 2 m) (ZMB 220002); Mpulungu Field Station (08°46.50′S, 31°05.005′E, 7 m) (ZMB 220046); Kasakalawe (08°47.480′S, 31°04.494′E, 4–5 m) (ZMB 220078).

Shell. Specimens examined (see Fig. 1A) ranging in height from 3.94 to 9.25 mm, on average 6.57 ± 1.47 mm (n = 46). Transition between protoconch and teleoconch gradual, indistinct (Fig. 1B). Sculpture of apical cap and first ~1.3 whorls more or less smooth, textured with irregular shallow pits and irregular spiral striations. Gradual transition to teleoconch sculpture consisting of fine, weakly opisthocyrt growth lines. Shell microstructure (Fig. 1C) consisting of one thick layer of crossed lamellar structure, bounded by thin outer irregular, prismatic and inner regular, simple prismatic layers.

External anatomy. Operculum (Fig. 2A) thin and delicate, transparent, light amber brown in colour. Operculum weakly paucispiral, comprising approximately 4.5 whorls with small, smooth, central nucleus; initial four whorls increasing evenly in size, last one-half whorl slightly flaring.

Foot ovate (Fig. 2B: f), tapering to slightly pointed posterior tip. Propodium narrow with pedal gland along anterior margin (Fig. 2B: ap). In females, small ovipositor (Fig. 2B: ovp) on right side of foot, below right eye, just above foot sole margin. Aperture of ovipositor forming simple, sinuous, oblique slit situated on slight rise. Ciliated egg groove between ovipositor and pallial oviduct lacking; lightly pigmented strip occasionally visible on neck and side of foot adjacent to ovipositor in some specimens. Ovipositor pore extending medially into foot, surrounded by muscle fibres. Pore lined with abundant goblet cells and ciliated, tall prismatic secretory cells with granular cytoplasm and staining light purple with haematoxylin & eosin; subepithelial glands lacking. Proximally, pore epithelium thrown into many even, fine folds (Fig. 6A). Further into foot, pore lumen expanding irregularly with onset of large anterodorsal fold. Pore lumen becoming briefly tripartite with three opposing folds (Fig. 6B), before dorsal fold becoming dominant and lumen becoming U-shaped (Fig. 6C: d.f).

Retracted cephalic tentacles (Fig. 2B,C: t) rather smooth, long and tapering, slightly longer than snout. Eyes located on small protuberances at base of tentacles. Extensible snout (Fig. 2D: sn) triangular, tapering to small mouth opening at tip; surface of snout and head only weakly grooved when retracted.

Mantle cavity extending approximately three-quarter whorls. Hypobranchial gland rather well developed (Fig. 2C: hg), with transverse grooves. Dorsal and lateral mantle edge (Fig. 3A: me) weakly fringed; in some specimens, fringe slightly thicker at inhalant margin adjacent to left cephalic tentacle. Ctenidium (Fig. 3A: ct) approximately one-third whorl in length, extending from near mantle margin almost to rear of mantle cavity; anterior tip of ctenidium curving slightly to the left. Gill with ~79–80 leaflets (n = 2); leaflets broadly triangular with projecting apices aligned along midline. Osphradium (Fig. 3A: os) short and thick, approximately one-quarter of ctenidium in length, sitting on surface of mantle roof (i.e. not within depression). Osphradium with two lightly pigmented, undulating ridges alongside central axis.

Alimentary system – Foregut. Radula taenioglossate with approximately 47–54 rows (n = 2 adults). Rachidian (Fig. 4A–C) quadrangular, wider than tall, with slightly rounded lateral edges, tapering to V-shaped lower margin. Upper margin slightly concave with cutting edge bearing prominent, central, sharply pointed cusp bounded by approximately five pointed denticles on each side. Lateral teeth with long lateral extensions, ~2.5–3 times length of cutting edge (Fig. 4A). Single, sharp prominent cusp flanked by three to four inner and four to six outer pointed denticles (Fig. 4B). Denticles of rachidian and lateral teeth smooth and decreasing in size toward outer edges of tooth. Denticle number and shape variation observed within and between individuals. Marginal teeth with long, slender simple shafts and broadly rounded cutting edges bearing approximately equal numbers (~13) of smooth, pointed denticles; denticles decreasing slightly in size toward outer margins of cutting edge (Fig. 4D).

Mouth opening ventrally at anterior end of snout. Buccal mass (Fig. 3A: bm) narrow, elongate, rather delicate; small

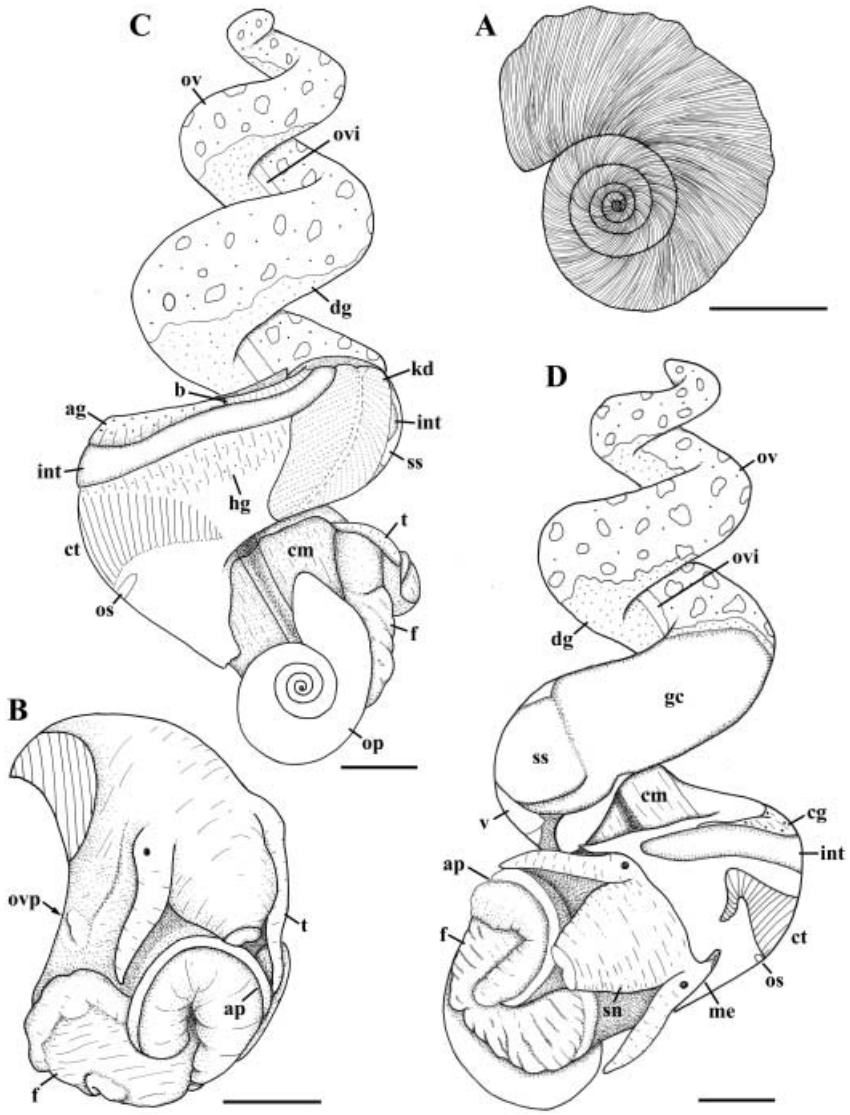

Fig. 2—External anatomy of *Syrnolopsis lacustris* (ZMB 220078). —**A**. Operculum. —**B**. Ovipositor. External view of head–foot of female. Note lightly pigmented strip on side of foot between ovipositor and cephalic tentacle. Cross-hatching indicates cross-section through columellar muscle. —**C, D**. External anatomy. External view of female removed from shell. Dotted line in kidney roof (C) indicates extent of pericardium. Abbreviations: ag, albumen gland; ap, anterior pedal gland; b, bladder; cg, capsule gland; cm, columellar muscle; ct, ctenidium; dg; digestive gland; f, foot sole; gc, gastric chamber of midgut; hg, hypobranchial gland; int, intestine; kd, main kidney chamber; me, mantle edge; op, operculum; os, osphradium; ov, ovary; ovi, oviduct; ovp, ovipositor; sn, snout; ss, style sac; t, cephalic tentacle; v, ventricle. Scale bars, 0.5 mm.

odontophore occupying posterior half of buccal cavity. Narrowly triangular, glandular subradular organ extending along floor of buccal cavity at anterior end of odontophore. Small, paired jaw dorsally flanking mouth. Shallow, non-glandular buccal pouches extending underneath dorsal folds adjacent to buccal ganglia at rear of buccal cavity. Salivary glands (Fig. 3A: sg) forming short, coiled, unbranched tubules, opening dorsolaterally alongside odontophore; salivary glands not extending through circumoesophageal nerve ring (Fig. 3A: nr). Thick buccal retractors (Fig. 3A: rt) extending from rear wall of buccal mass, inserting on lateral walls of cephalic haemocoele just in front of nerve ring (Fig. 3A: nr). Nerve ring lying short distance back from posterior end of buccal mass. Radular sac short, projecting slightly past end of buccal mass and curving dorsally underneath anterior oesophagus. Within anterior oesophagus, short, glandular mid-ventral fold just behind odontophore. Paired ventral longitudinal folds commencing immediately behind mid-ventral fold; walls of anterior oesophagus bearing paired, longitudinal ventral and dorsal folds with intervening glandular epithelium bearing scattered goblet cells (Fig. 3A). Mid-oesophageal gland lacking. Below base of mantle cavity, posterior mid-oesophagus coiled. Posterior oesophagus narrowing below pericardium.

Alimentary system – Midgut. Oesophagus opening anteriorly to left side of gastric chamber floor (Fig. 3B: e). Marginal fold (Fig. 3B: mf) extending anteriorly from oesophageal aperture alongside expanded proximal tip of major typhlosole (Fig. 3B: t1), then turning posteriorly bordering margin of sorting area (Fig. 3B: sa). Sorting area triangular, with straight left margin and tapering to pointed, slightly curving posterior tip. Small, rounded pad (Fig. 3B: sap) at left, posterior tip of sorting area. Accessory marginal fold

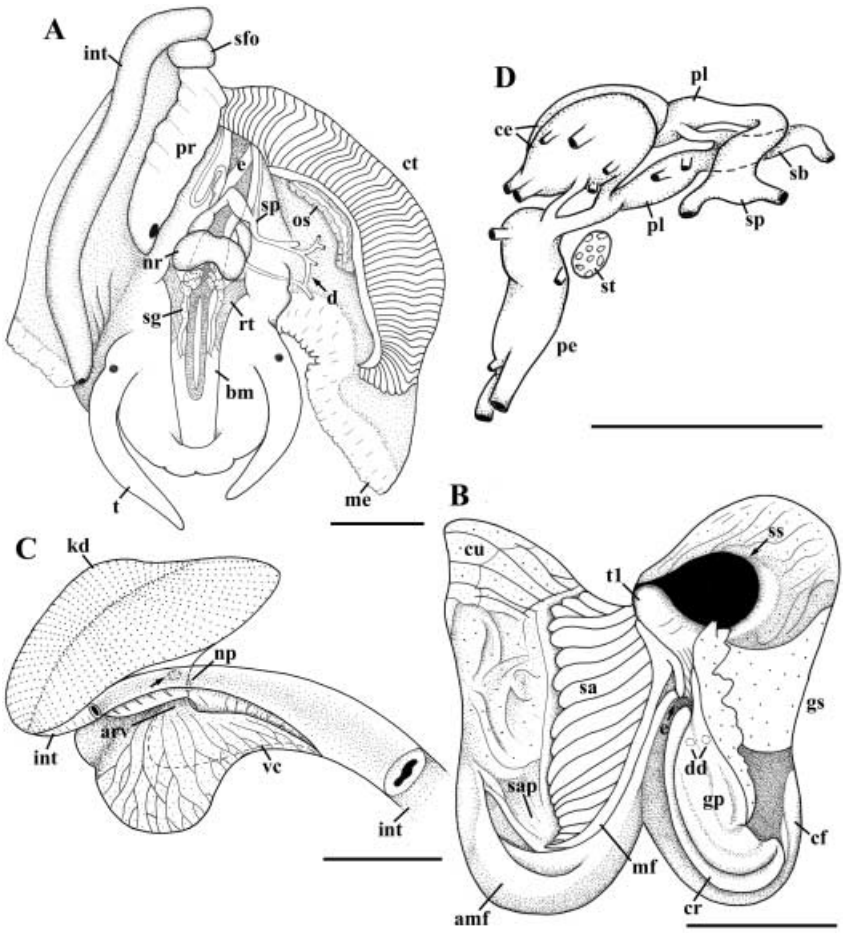

Fig. 3—External and internal anatomy of *Syrnolopsis lacustris* (ZMB 220078). —**A**. Mantle cavity and cephalic haemocoele. Dorsal view, anterior is below. Hypobranchial gland has been removed. Stippling in buccal cavity, anterior and mid-oesophagus indicates glandular epithelium between paired dorsal and ventral folds. —**B**. Midgut. Dorsal view, anterior is uppermost. —**C**. Kidney. Internal view of bladder. Lateral view, anterior is to the right. Right wall of bladder cut along ventral edge of intestine and deflected laterally to reveal interior; segment of intestine removed for greater visibility. Arrow indicates opening allowing communication between bladder and main kidney chamber. Dotted line indicates extent of ventral chamber. Note that main kidney chamber appears foreshortened in this view, as it curves ventrally to the left. —**D**. Circumoesophageal nerve ring. Left lateral view, anterior is to the left. Abbreviations: amf accessory marginal fold; arv, afferent renal vessel; bm, buccal mass; ce, cerebral ganglion; cf, caecal fold; cr, crescentic ridge; ct, ctenidium; cu, cuticularized region of stomach roof; d, dialyneury; dd, duct of digestive gland; e, oesophagus; gp, glandular pad; gs, gastric shield; int, intestine; kd, main kidney chamber; me, mantle edge; mf, marginal fold; np, nephropore; nr, circumoesophageal nerve ring; os, osphradium; pe, pedal ganglion; pl, pleural ganglion; pr, prostate; rt, buccal mass retractor muscle; sa, sorting area; sap, sorting area pad; sb suboesophageal ganglion; sfo, spermatophore-forming organ; sg, salivary gland; sp, supraoesophageal ganglion; ss, lip of style sac; st, statocyst; t, cephalic tentacle; t1, major typhlosole; vc, ventral kidney chamber. Scale bars, 0.5 mm.

(Fig. 3B: amf) emerging from oesophageal aperture, paralleling marginal fold and curving around posterior tip of sorting area; accessory marginal fold bifurcate posteriorly. Epithelium of gastric chamber floor finely grooved anterior to oesophagus, at right of marginal fold. Gastric shield (Fig. 3B: gs) large, concave, with coarsely serrated left margin; shield continuous with cuticle lining gastric chamber roof (Fig. 3B: cu) and region around style sac aperture. Cuticularized region in roof (Fig. 3B: cu) coarsely, transversely folded anteriorly, rather smooth posteriorly. Shield supported at left by large, elongately rounded glandular pad (Fig. 3B: gp); accessory pad and caecum lacking. Crescentic ridge (Fig. 3B: cr) extending from oesophageal aperture and fusing to right, posterior end of glandular pad. Proximal tip of crescentic ridge bounding deep pocket bearing two digestive gland duct apertures (Fig. 3B: dd). Two weak, longitudinal folds (Fig. 3B: cf) along gastric chamber floor behind shield. Style sac (Fig. 3B: ss) communicating proximally with intestine. Crystalline style present.

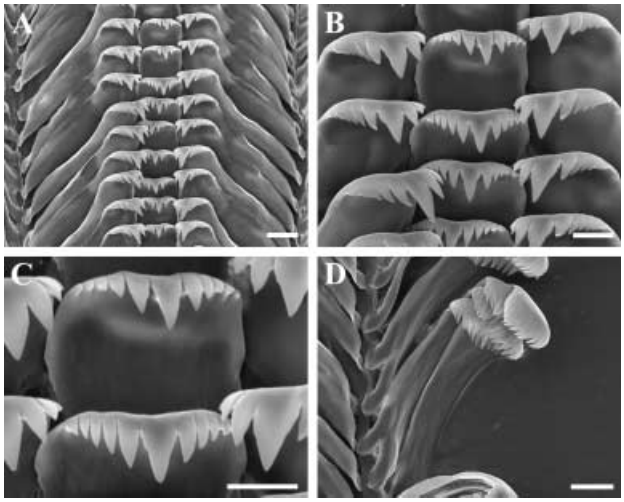

Fig. 4—Radula of *Syrnolopsis lacustris* (ZMB 220078). —**A**. Rachidian and lateral teeth. Scale bar, 10 μm. —**B**. Detail of cutting edge of rachidian and lateral teeth. Scale bar, 5 μm. —**C**. Detail of rachidian cutting edge. Scale bar, 5 μm. —**D**. Marginal teeth. Scale bar, 10 μm.

Within gastric chamber, mucus and unidentifiable organic debris mixed with small, angular, quartzose sand grains.

Alimentary system – Hindgut. Proximal intestine separating from style sac, curving underneath distal tip of style sac (Fig. 2D: ss), and forming short recurvent segment (Fig. 2C: int) alongside style sac at rear end of kidney. Intestine continuing forward under posterior end of kidney (Fig. 2C: kd), entering pallial roof between bladder (Fig. 2C: b) and main kidney chamber (Fig. 2C: kd), to papillate anus near mantle margin.

Reno-pericardial system. Kidney forming three interconnected chambers (Figs 2C and 3C). Main chamber (Figs 2C and 3C: kd) lying obliquely across axis of body from right to left, bounding distal half of style sac at right, dorsally surrounding pericardium (Fig. 2C), extending short distance into pallial roof at base of mantle cavity. Main chamber roughly T-shaped in cross-section, narrowing alongside pericardium from broad, flat roof; chamber largely occluded with excretory tubules. Below main chamber, second chamber forming voluminous bladder (Fig. 2C: b), reaching from pericardium to right body wall below intestine (Fig. 3C, exposed chamber), extending short distance into mantle roof between intestine and pallial gonoduct. Bladder subdivided horizontally by shallow sheet of excretory tissue extending from near nephropore (Fig. 3C: np) to rear wall. Excretory tissue on bladder walls varying considerably in thickness between individuals, occasionally forming thick anastomosing network along right wall and below intestine floor. Excretory tissue separating small ventral chamber below (Fig. 3C: vc). Small aperture (Fig. 3C) just behind afferent renal vessel (Fig. 3C: arv) connecting main chamber and bladder. Bladder communicating to mantle cavity via small nephropore. Nephridial gland absent.

Pericardium deep and voluminous, extending to midline of main kidney chamber (Fig. 2C); large auricle and ventricle (Fig. 2D: v) almost filling pericardial lumen.

Nervous system. Circumoesophageal nerve ring condensed, with ganglia joined by short connectives and commissures (Fig. 3D). Cerebral ganglia (Fig. 3D: ce) separated by slight constriction; each ganglion producing six nerves, including small statocyst nerve. Buccal connectives short, innervating buccal ganglia lying ventrolaterally at base of buccal cavity immediately behind radular sac. Pleural ganglia (Fig. 3D: pl) slightly behind and below cerebral ganglia; left pleural ganglion producing two small nerves, including pallial nerve. Pedal ganglia (Fig. 3D: pe) with two prominent anterior nerves and three smaller accessory nerves. Small statocysts (Fig. 3D: st) with numerous statoconia present dorsally, alongside pedal ganglia behind pedal connectives. Suboesophageal ganglion (Fig. 3D: sb) lying slightly to right of midline, connected to left pleural ganglion by short connective. Zygoneury formed between suboesophageal and right pleural ganglia. In addition to nerve joining right pleural ganglion, suboesophageal ganglion producing one prominent nerve with a small branch near its origin. Short, thick connective uniting right pleural and supraoesophageal (Fig. 3D: sp.) ganglia. Left dialyneury (Fig. 3A: d) formed between pallial nerve of left pleural ganglion and nerve from supraoesophageal ganglion at junction of mantle roof and floor. Single visceral ganglion below pericardium at base of mantle cavity, to right of posterior oesophagus; ganglion producing two nerves.

Reproductive system – Female. Gonad (Fig. 2D: ov) dorsally overlying digestive gland (Fig. 2D: dg) from tip of visceral mass to posterior end of gastric chamber (Fig. 2D: gc). Oviduct (Fig. 2D: ovi) emerging ventrally from ovary and extending forward along ventral midline. Oviduct (Fig. 5A–C: ovi) forming recurvent loop before entering rear of glandular pallial oviduct at base of mantle cavity. Pallial oviduct forming simple, straight, flattened tube with proximal albumen (Fig. 5A–C: ag) and distal capsule glands (Fig. 5A–C: cg); albumen gland forming roughly one-third and capsule gland approximately two-thirds of pallial oviduct. Epithelium of capsule and albumen glands irregularly transversely segmented; segmentation more distinctly developed within capsule gland. Small, slit-like anterior aperture (Fig. 5A) opening to elongate spermatophore bursa (Fig. 5A: spb) lying within medial lamina. Spermatophore bursa containing unorientated sperm, communicating to capsule gland through long slit (Fig. 5C) between overlapping

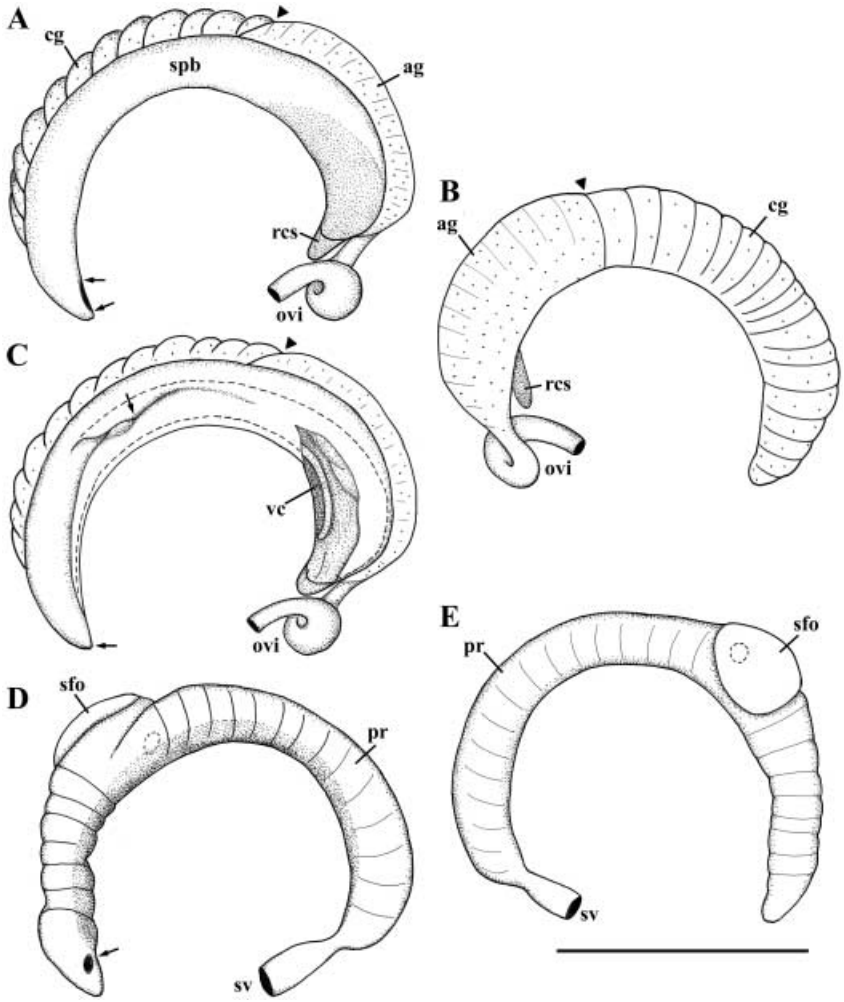

Fig. 5—Reproductive anatomy of *Syrnolopsis lacustris* (ZMB 220078). —**A**. External, left lateral view of pallial oviduct. Anterior is to the left. Arrows indicate extent of opening between mantle cavity and spermatophore bursa; arrowheads indicate transition between albumen and capsule glands. Stippling in posterior portion of bursa indicates the presence of orientated sperm seen by transparency within seminal receptacle; note posterior tip of receptacle projecting past tip of bursa. —**B**. External, right lateral view of pallial oviduct. Anterior is to the right. —**C**. Internal view of pallial oviduct. Front wall and posterior portion of inner wall of spermatophore bursa removed, revealing communication between bursa and gonoductal groove (arrows), as well as internal surface of seminal receptacle and communication with ventral channel. —**D**. External, left lateral view of prostate. Anterior is to the left. Dotted line indicates communication between spermatophore-forming organ and prostate. Arrow indicates anterior opening to mantle cavity. —**E**. External, right lateral view of prostate. Anterior is to the right. Dotted line indicates communication between spermatophore-forming organ and prostate. Abbreviations: ag, albumen gland; cg, capsule gland; ovi, oviduct; pr, prostate; rcs, seminal receptacle; sfo, spermatophore-forming organ; spb spermatophore bursa; sv, seminal vesicle; vc, ventral channel. Scale bar, 1 mm.

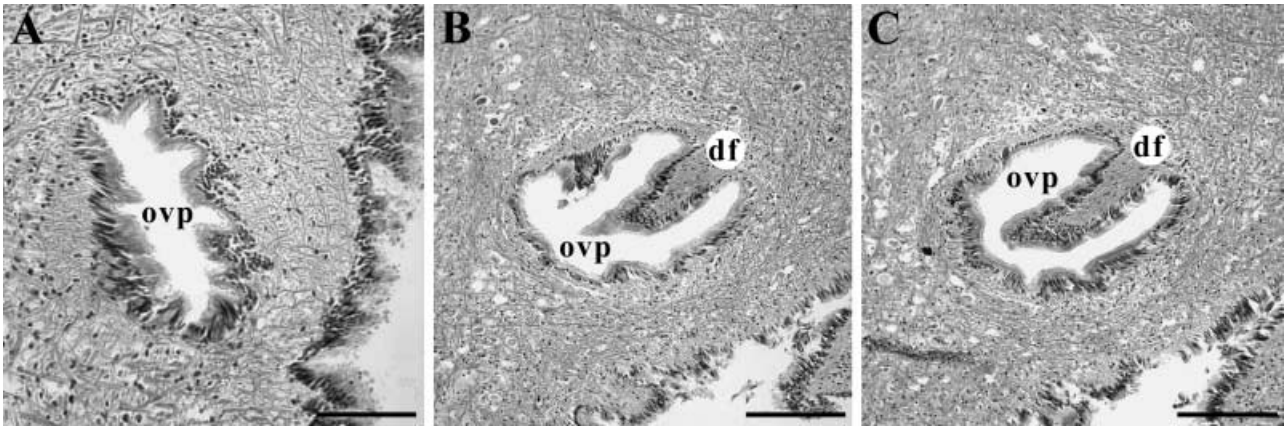

Fig. 6—Histology of the ovipositor of *Syrnolopsis lacustris* (ZMB 220078). —**A**. Proximal pore with many fine folds. Scale bar, 50 μm. —**B**. Mid-pore with three opposing folds. Scale bar, 100 μm. —**C**. Inner pore with single dominant dorsal fold. Scale bar, 100 μm. Abbreviations: ovp, lumen of ovipositor pore; df, dorsal fold.

dorsal and ventral folds. Dorsal fold represents free inner wall of medial lamina; ventral fold arising from ventral channel short distance back from anterior tip of gonoduct. One-third of oviduct length from anterior tip, dorsal fold forming small lateral projection quickly fusing with ventral fold, sealing communication between bursa and gonoductal groove. Dorsal fold continuing posteriorly, separating median chamber along inner wall of bursa; chamber functioning as seminal receptacle (Fig. 5A,B: rcs). Receptacle communicating ventrally with ventral channel (Fig. 5A,B: vc). Near posterior tip of gonoduct, dorsal wall fusing with ventral channel, forming blind posterior tip of receptacle containing orientated sperm. Tip of receptacle extending only short distance beyond end of spermatophore bursa.

Reproductive system – Male. Vas deferens emerging ventrally from testes, continuing forward along ventral midline of whorl. Straight, distal vas deferens swollen with ripe sperm and functioning as seminal vesicle (Fig. 5D,E: sv). Vas deferens constricting slightly before entering posterior end of prostate (Fig. 5D,E: pr) at base of mantle cavity. Prostate forming narrow, glandular tube, communicating with mantle cavity through small anterior aperture (Fig. 5D). Prostate opening to small, glandular pouch-like spermatophore forming organ (Fig. 5D,E: sfo). Organ communicating posteriorly with gonoduct via small, rounded aperture (Fig. 5E). Within gonoduct, aperture bounded dorsally by large, longitudinal glandular fold extending anteriorly from aperture along wall of lateral lamina; fold roughly equal in length to spermatophore organ. Glandular tissue of lateral and medial laminae transversely segmented along entire length; in some specimens, segmentation becoming weaker and less regular anteriorly and in region surrounding large glandular fold. Glands of prostate acidophilic posteriorly and becoming strongly basophilic within spermatophore organ and in glands of prostate in region alongside spermatophore organ. From anterior end of spermatophore organ, glands of prostate becoming more acidophilic towards anterior tip of pallial gonoduct, expanding from ventral surface.

Anceya giraudi Bourguignat, 1885

Material examined. Tanzania: Kigoma (ZMB 220132). Zaire: Cap Banza (04°05′S, 29°10′E) (MNHN, 'sur beach-rock près du champ de sources') (MNHN, 'placers de sable, sous le site hydrothermal') (MNHN, 'sur beach-rock près du champ de sources'); Pemba (03°35′S, 29°08′E) (MNHN, 'substrat dûr autour des bouches hydrothermales') (MNHN, 'substrat rocheux'). Zambia: Kasenga Point (08°42.892′S, 31°08.463′E, 15+ m) (ZMB 220070) (08°42.887′S, 31°08.476′E, 20 m) (ZMB 220000); Kumbula Island (08°45.547′S, 31°05.825′E, 0–1 m) (ZMB 220106) (08°45.258′S, 31°05.116′E, 3 m) (ZMB 220049).

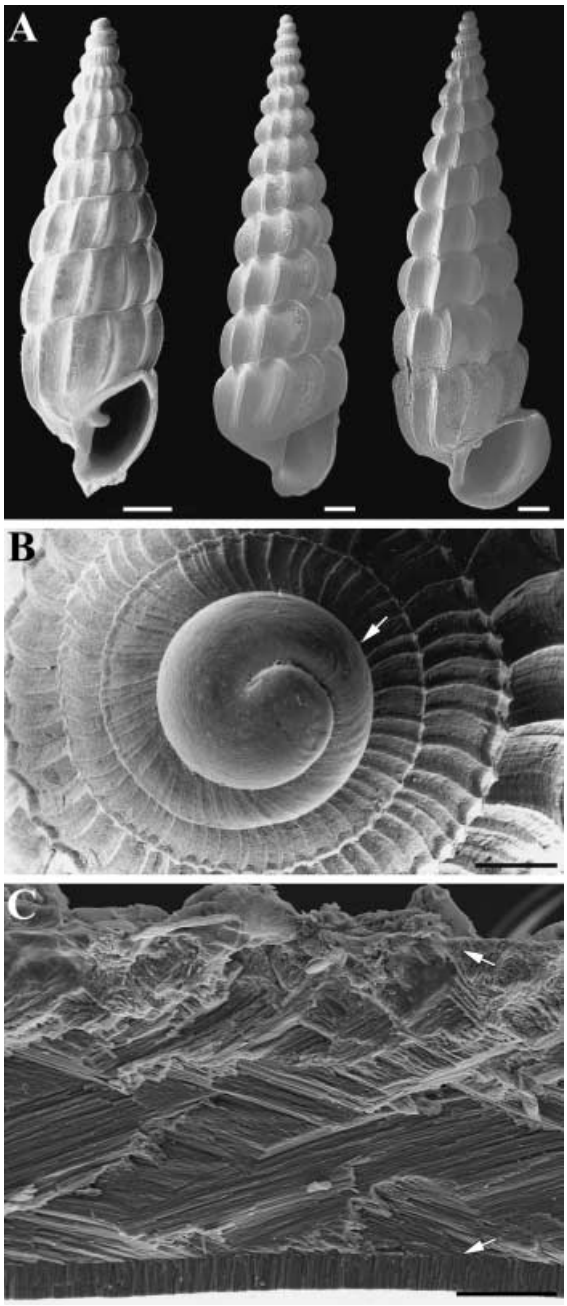

Fig. 7—Shell morphology of *Anceya giraudi* (unless noted, ZMB 220070). —**A**. Shell. Apertural view of shells. Note slight variation in height and spacing of axial ribs between individuals. Specimen on left is juvenile with aperture broken to reveal detail of columellar plait (ZMB 220132), middle specimen is young adult, specimen on right is adult with thickened, flaring aperture. Scale bars, 500 μm. —**B**. Protoconch (ZMB 220132). Apical view of protoconch with detail of radial sculpture and transition to axial sculpture of teleoconch. Arrow indicates transition between coarse radial sculpture and thick, undulating prosocline axial elements. Scale bar, 100 μm. —**C**. Microstructure. Cross-sectional view, shell exterior is uppermost. Arrows indicate transitions between layers. Scale bar, 20 μm.

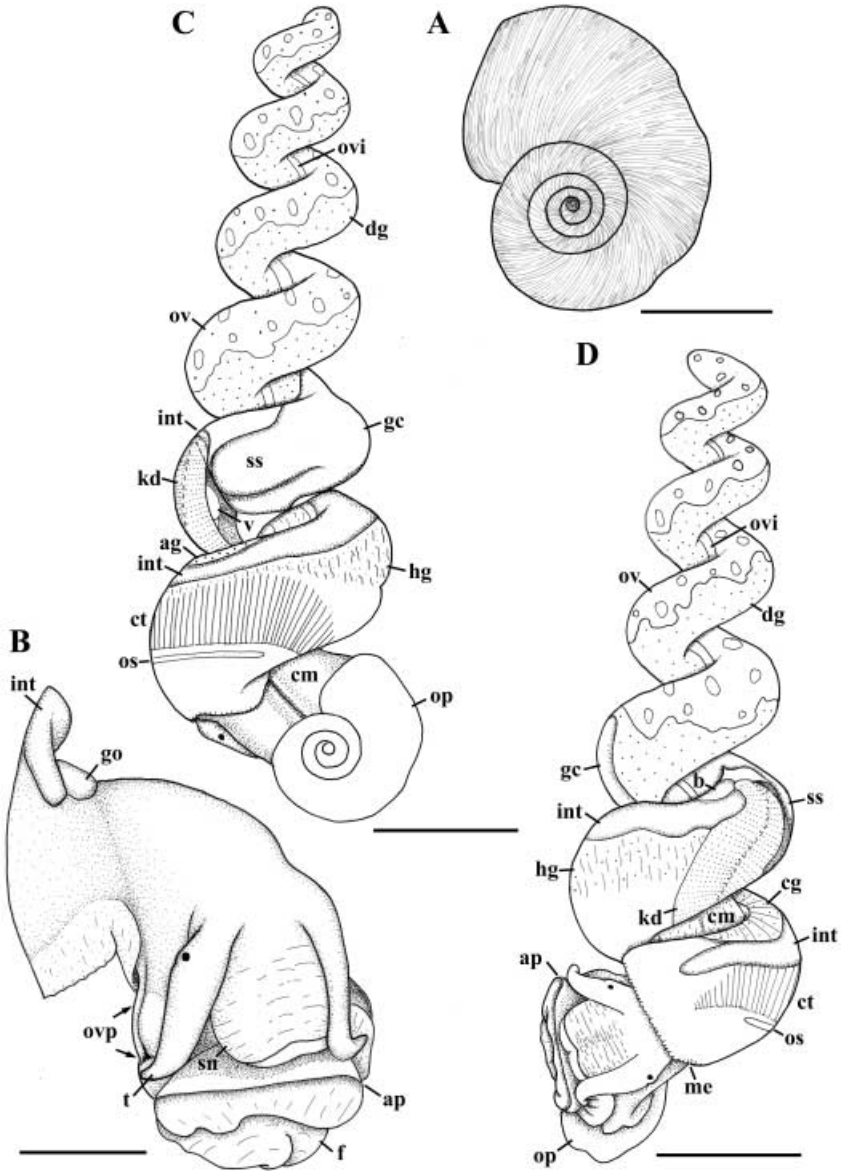

Fig. 8—External anatomy of *Anceya giraudi* (ZMB 220070). —**A**. Operculum. Scale bar, 0.5 mm. —**B**. Ovipositor. External view of head–foot of female. Arrows indicate length of pore. Scale bar, 0.5 mm. —**C, D**. External anatomy. External view of female removed from shell. Dotted line in kidney roof indicates extent of pericardium. Scale bars, 1 mm. Abbreviations: ag, albumen gland; ap, anterior pedal gland; b, bladder; cg, capsule gland; cm, columellar muscle; ct, ctenidium; dg; digestive gland; f, foot sole; gc, gastric chamber of midgut; hg, hypobranchial gland; int, intestine; kd, main kidney chamber; me, mantle edge; op, operculum; os, osphradium; ov, ovary; ovi, oviduct; ovp, ovipositor; sn, snout; ss, style sac; t, cephalic tentacle; v, ventricle. Scale bars, 0.5 mm.

Shell. Specimens examined (see Fig. 7A) ranging in height from 4.00 to 9.75 mm, on average 7.13 ± 1.17 mm (n = 143). Sculpture on apical cap (Fig. 7B) more or less smooth with some minor irregular undulations, followed by approximately one-half whorl of fine spiral striae; rapid transition to coarse, irregular spiral striae (roughly one-quarter whorl) followed by gradual transition (Fig. 7B) to thick, undulating prosocline axial elements interspersed with fine growth lines. On first half whorl of teleoconch, axial elements becoming gradually opisthocyrt and more sharply defined. On remaining whorls of teleoconch, axial elements gradually becoming more pronounced and decreasing in frequency.

Remarks. Shell microstructure (Fig. 7C) essentially identical to that of *S. lacustris*. Although the thickness of the shell, as well as of individual layers, differ between the two species, this can vary ontogenetically within individuals as well.

External anatomy. Operculum (Fig. 8A) comprising approximately four whorls. Aperture of ovipositor (Fig. 8B: ovp) forming short elongate slit on side of foot (Fig. 8B), situated on slight rise near foot sole; shallow groove extending short distance from pore along neck, almost to mantle margin. Pore narrowing from aperture medially into foot. Opposing anterodorsal and posteroventral folds rapidly developing, producing H-shaped lumen (Fig. 12A). Channels separated by folds gradually broadening. Distally, ventral fold becoming obsolete (Fig. 12B); near blind tip of pore, lumen simple, flattened with dorsal fold becoming obsolete (Fig. 12C). Mantle cavity long, narrow, extending just over one whorl.

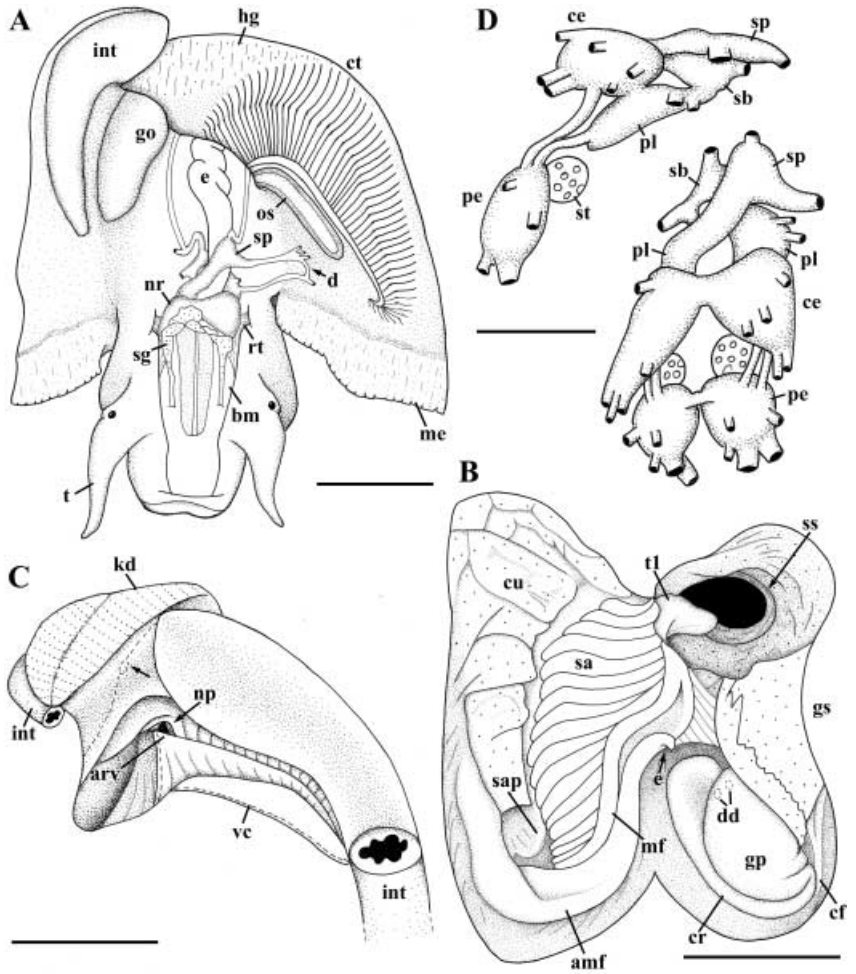

Fig. 9—External and internal anatomy of *Anceya giraudi* (ZMB 220070). —**A**. Mantle cavity and cephalic haemocoele. Dorsal view, anterior is below. Stippling in buccal cavity indicates glandular epithelium between dorsal folds. —**B**. Midgut. Dorsal view, anterior is uppermost. —**C**. Kidney. Internal view of bladder. Lateral view, anterior is to the right. Right wall of bladder cut along ventral edge of intestine and deflected laterally to reveal interior; segment of intestine removed for greater visibility. Arrow indicates opening allowing communication between bladder and main kidney chamber; adjacent dotted line indicates ventral extent of excretory tissue within main chamber. Dotted line below indicates extent of ventral chamber (vc). —**D**. Circumoesophageal nerve ring. Left lateral view above, anterior is to the left; dorso-frontal view below. Abbreviations: amf accessory marginal fold; arv, afferent renal vessel; bm, buccal mass; ce, cerebral ganglion; cf, caecal fold; cr, crescentic ridge; ct, ctenidium; cu, cuticularized region of stomach roof; d, dialyneury; dd, duct of digestive gland; e, oesophagus; go, pallial gonoduct; gp, glandular pad; gs, gastric shield; hg, hypobranchial gland; int, intestine; kd, main kidney chamber; me, mantle edge; mf, marginal fold; np, nephropore; nr, circumoesophageal nerve ring; os, osphradium; pe, pedal ganglion; pl, pleural ganglion; rt, buccal mass retractor muscle; sa, sorting area; sap, sorting area pad; sb suboesophageal ganglion; sg, salivary gland; sp, supraoesophageal ganglion; ss, lip of style sac; st, statocyst; t, cephalic tentacle; t1, major typhlosole; vc, ventral kidney chamber. Scale bars, 0.5 mm.

Dorsal and lateral mantle edge (Fig. 9A: me) evenly fringed. Ctenidium (Fig. 9A: ct) long, approximately one-half whorl in length, extending from near mantle margin, terminating well forward of mantle cavity base. Gill with ~59–60 leaflets (n = 2); leaflet profile variable, but typically low, broadly triangular, with projecting apices aligned near midline. Osphradium approximately one third of gill in length.

Remarks. In contrast to *S. lacustris*, and to some extent reflecting differences in shell shape, overall the animal is much more slender and also fills a larger volume within the shell. Thus, the body of *A. giraudi* individuals comprises a greater numbers of whorls, with slightly more than four whorls occupied by digestive gland and gonad and ~2.5 whorls occupied by the (retracted) head–foot and organs of the viscera; the magnitude of these differences vary with maturity and hence size and development of the gonad. The propodium is broader with a correspondingly longer anterior pedal gland (Fig. 8B: ap). Ctenidial leaflets have a lower profile, with projecting apices aligned slightly off centre,

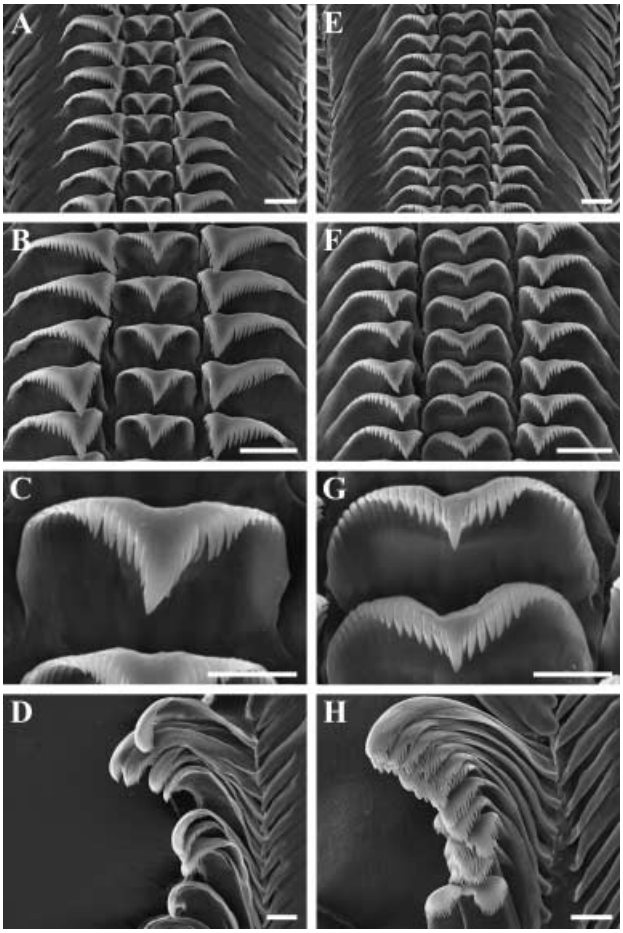

Fig. 10—Radula of *Anceya giraudi* (ZMB 220070). —**A**–**D**. Detail of radula from one individual. —**E**–**H**. Detail of radula from second individual. —**A**, **E**. Rachidian and lateral teeth. Scale bars, 10 μm. —**B**, **F**. Detail of cutting edge of rachidian and lateral teeth. Scale bars, 10 μm. —**C**, **G**. Detail of rachidian cutting edge. Scale bars, 5 μm. —**D**, **H**. Marginal teeth. Scale bars, 10 μm.

shifted toward the efferent branchial vein. The osphradium is longer, extending approximately two-thirds to three-quarters the length of the ctenidium. Similar to *S. lacustris*, the osphradium forms two lateral ridges along a central axis, but the lateral ridges are smooth, not undulating.

The ovipositor pore, while similar in the details of the glandular epithelium, differs in that it narrows considerably upon entering the foot. Additionally, the pattern of folds within the pore is primarily H-shaped, rather than U-shaped.

Alimentary system – Foregut. Radula with approximately 57–76 rows (n = 3 adults). Rachidian (Fig. 10A–H) rectangular, wider than tall, with slightly rounded lateral edges, tapering to V-shaped lower margin. Upper margin slightly concave with cutting edge bearing narrow, central, sharply pointed cusp bounded by ~13–16 fine, pointed denticles on each side. Lateral teeth with long lateral extensions, ~2.5–3 times length of cutting edge (Fig. 10A,E). Single, narrow, sharp prominent cusp flanked by ~10–12 inner and ~15–18 outer finely pointed denticles (Fig. 10B,F). Denticles of rachidian (Fig. 10C,G) and lateral teeth smooth, decreasing in size toward outer edges of tooth; denticle patterns, including shape and size of denticles and fusion of adjacent denticles, highly variable within and between individuals. Inner and outer marginal teeth similar, with long, slender simple shafts and broadly rounded cutting edges bearing numerous finely fringed pointed denticles (Fig. 10D,H).

Alimentary system – Midgut. Glandular pad short, rounded, thick (Fig. 9B: gp). Caecal fold single, bifurcating anteriorly (Fig. 9B: cf).

Remarks. The radula of *A. giraudi* differs from that of *S. lacustris* in the shape of the rachidian, size and number of denticles flanking the prominent central cusps on the rachidian and lateral teeth, and size and number of denticles on the marginal teeth. Although the sample size is small, individuals of *A. giraudi* apparently display more variation in cusp patterns within and between individuals.

The buccal mass (Fig. 9A: bm) and odontophore of *A. giraudi* are slightly more robust, but the configuration of the salivary gland ducts (Fig. 9A: sg) and the folds in the anterior oesophagus are identical to *S. lacustris*.

The midgut, apart from minor individual variation, is essentially identical between the two species. The most significant differences are the thickness of the accessory marginal fold (Fig. 9B: amf), size and shape of the glandular pad (Fig. 9B: gp), and the pattern of caecal folds (Fig. 9B: cf). The course of the hindgut is also essentially identical between the two. However, in *S. lacustris*, the recurvent segment of the intestine is longer, roughly one-third the length of the style sac (Fig. 2C: int, ss), whereas in *A. giraudi*, the intestine just embraces the distal tip of the style sac (Fig. 8C: int, ss). The rectum (Fig. 9A: int) in the latter species occurs well back from the mantle edge, near the anterior end of the pallial gonoduct (Fig. 9A: go).

Reno-pericardial system.

Remarks. Configuration of the kidney is identical between the two species, but in *A. giraudi* the intestine is broader where it traverses the kidney. Correspondingly, the bladder (Fig. 9C) and the vertical limb of the main kidney chamber are taller and hence, more voluminous. Individuals of both species display marked variation in excretory tissue development.

Nervous system. Buccal commissure very short; buccal ganglia ventral, between anterior oesophagus and radular sac.

Remarks. Like *S. lacustris*, *A. giraudi* is characterized by six cerebral nerves and a zygoneurous connection between the right pleural and suboesophageal ganglia (Fig. 9D).

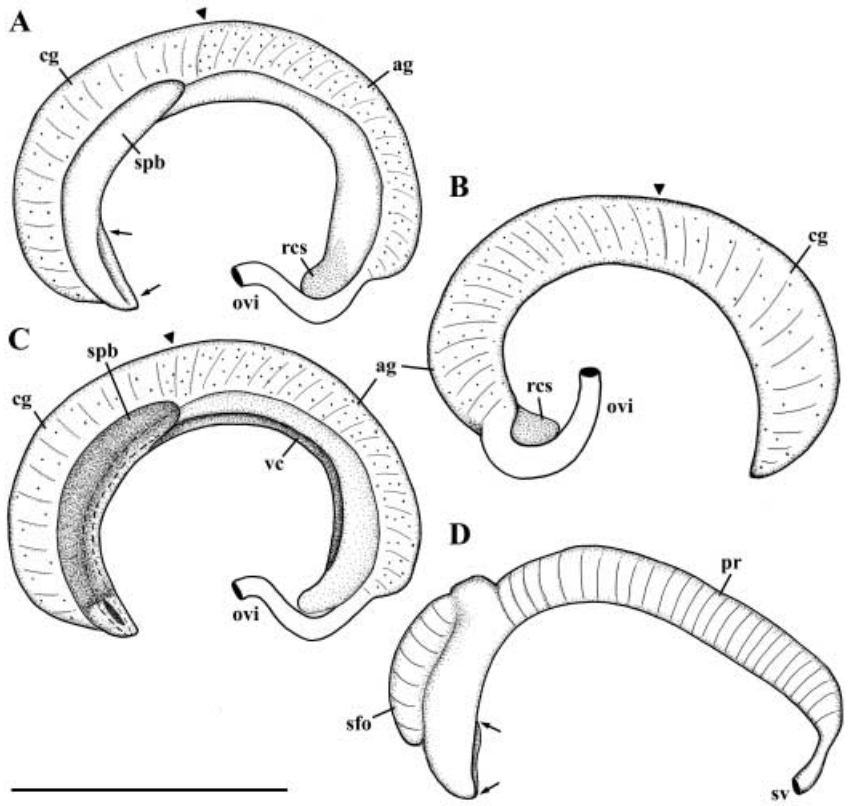

Fig. 11—Reproductive anatomy of *Anceya giraudi* (ZMB 220070). —**A**. External, left lateral view of pallial oviduct. Anterior is to the left. Arrows indicate extent of opening between mantle cavity and spermatophore bursa; arrowheads indicate transition between albumen and capsule glands. —**B**. External, right lateral view of pallial oviduct. Anterior is to the right. —**C**. Internal view of pallial oviduct. External walls of spermatophore bursa and seminal receptacle removed. —**D**. External, left lateral view of prostate. Anterior is to the left. Arrows indicate extent of opening between mantle cavity and gonoductal groove. Abbreviations: ag, albumen gland; cg, capsule gland; ovi, oviduct; pr, prostate; rcs, seminal receptacle; sfo, spermatophore-forming organ; spb spermatophore bursa; sv, seminal vesicle; vc, ventral channel. Scale bar, 1 mm.

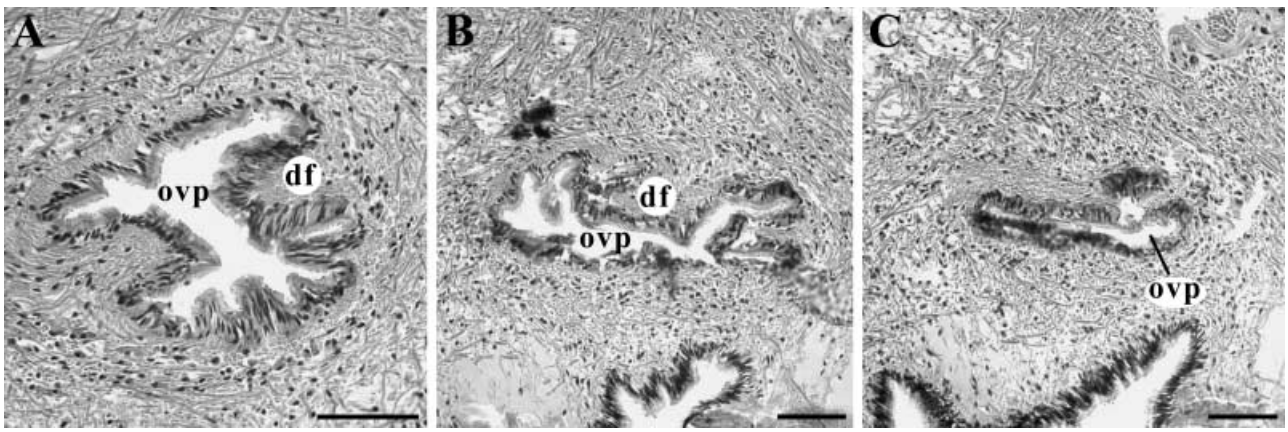

Fig. 12—Histology of the ovipositor of *Anceya giraudi* (ZMB 220070). —**A**. Proximal pore with H-shaped lumen. —**B**. Mid-pore with single dominant dorsal fold. —**C**. Inner pore forming simple flattened lumen. Abbreviations: ovp, lumen of ovipositor pore; df, dorsal fold. Scale bars, 50 μm.

Reproductive system – Female. Albumen (Fig. 11A,B: ag) and capsule glands (Fig. 11A,B: cg) each occupying roughly one-half of pallial oviduct, but albumen gland slightly longer. Elongate, slit-like anterior aperture (Fig. 11A) opening to spermatophore bursa (Fig. 11A: spb); bursa roughly equal to capsule gland in length. Bursa communicating with capsule gland through short, narrow anterior slit (Fig. 11C). Seminal receptacle forming blind posterior extension of ventral channel.

Reproductive system – Male. Prostate forming narrow, glandular tube (Fig. 11D: pr), communicating with mantle cavity through slit-like anterior aperture (Fig. 11D). Prostate communicating dorsally at anterior one-third, via small

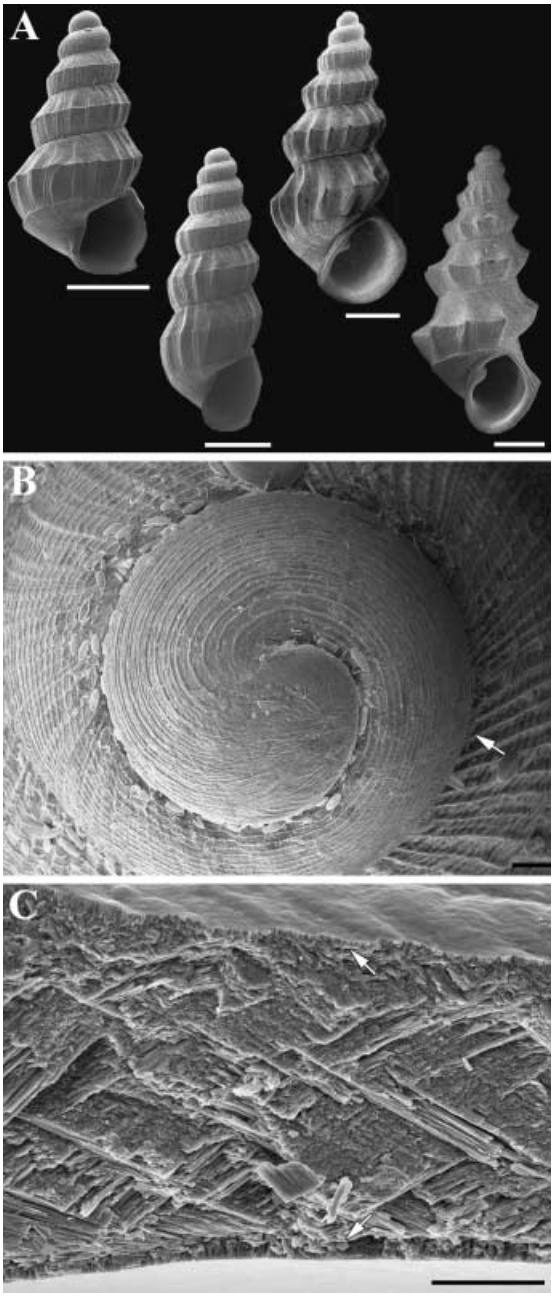

Fig. 13—Shell morphology of *Martelia tanganyicensis* (except when noted, ZMB 220006). —**A**. Shell. Apertural view of shells. Note variation in shell width and development of columellar plait, carina and axial ribs. Two specimens on left are young adults; two specimens on right are adults with thickened apertures. Shell second from left from lot ZMB 220133. Scale bars, 500 μm. —**B**. Protoconch. Apical view of protoconch with detail of spiral and axial threads. Arrow indicates onset of visible axial growth lines between radial threads. Scale bar, 20 μm. —**C**. Microstructure. Cross-sectional view, shell exterior is uppermost. Arrows indicate transitions between internal crossed-lamellar layer and outer irregular, prismatic and inner regular, simple prismatic layers. Scale bar, 10 μm.

aperture, with elongate, tubular spermatophore forming organ (Fig. 11D: sfo); longitudinal glandular fold bounding aperture lacking. Glandular tissue of lateral and medial laminae and spermatophore organ transversely segmented; segmentation obsolete in anterior one-third of prostate. Posterior prostate strongly acidophilic and becoming slightly more basophilic nearer to spermatophore organ. In region of communication between spermatophore organ and prostate, epithelium basophilic; anterior to junction, epithelium of prostate again becoming slightly more acidophilic. Epithelium of spermatophore organ basophilic.

Remarks. Female reproductive anatomy of *A. giraudi* and *S. lacustris* differs in that the albumen and capsule glands comprise slightly different proportions of the gonoduct, the bursa is much shorter in *A. giraudi*, communication between the bursa and capsule gland is considerably longer in *S. lacustris*, while the aperture leading from the mantle cavity to the bursa is slightly longer in *A. giraudi*. Additionally, in the specimens of *A. giraudi* observed, sperm storage was primarily restricted to the blind tip of the receptacle rather than expanding anteriorly to the region above the opening to the ventral channel as in *S. lacustris*.

The spermatophore-forming organs of *A. giraudi* and *S. lacustris* differ in that the former is similar to that of other Lake Tanganyika paludomids (see e.g. Strong and Glaubrecht 2002, 2003; Glaubrecht and Strong 2004), while that of the latter has been reduced to a small rounded pouch. Additionally, the aperture allowing communication between the mantle cavity and gonoduct is much smaller in *S. lacustris*. While the precise details differ slightly, distribution of acidophilic and basophilic glands within the prostate are generally similar; in both, the spermatophore organ is strongly basophilic.

Martelia tanganyicensis Dautzenberg, 1908

Material examined. Zambia: Kumbula Island (08°45.258′S, 31°05.116′E) (ZMB 220006, 220041); (08°45.547′S, 31°05.825′E) (ZMB 220067). Tanzania: Kigoma (ZMB 220134, 220133). Zaire: Cap Banza (04°05′S, 29°10′E) (MNHN, 'placers de sable, sous le site hydrothermal') (MNHN, 'sur beach-rock près du champ de sources'); Pemba (03°35′S,29°08′E) (MNHN, 'substrat dûr autour des bouches hydrothermales') (two lots).

Shell. Specimens examined (see Fig. 13A) ranging in height from 1.60 to 4.14 mm, on average 3.07 ± 0.56 mm (n = 80). Sculpture on apical cap (Fig. 13B) of fine, irregular spiral striae. Rapid transition to numerous spiral threads interspersed with irregular striae. Fine growth lines appearing at ~1.3 whorls; at ~1.625 whorls, irregularly spaced prosocline axial threads appearing, rapidly becoming opisthocyrt and more prominent; small nodes forming at intersection of axial and spiral elements. Second teleoconch whorl becoming carinate at midline of whorl, with prominent spiral cord along

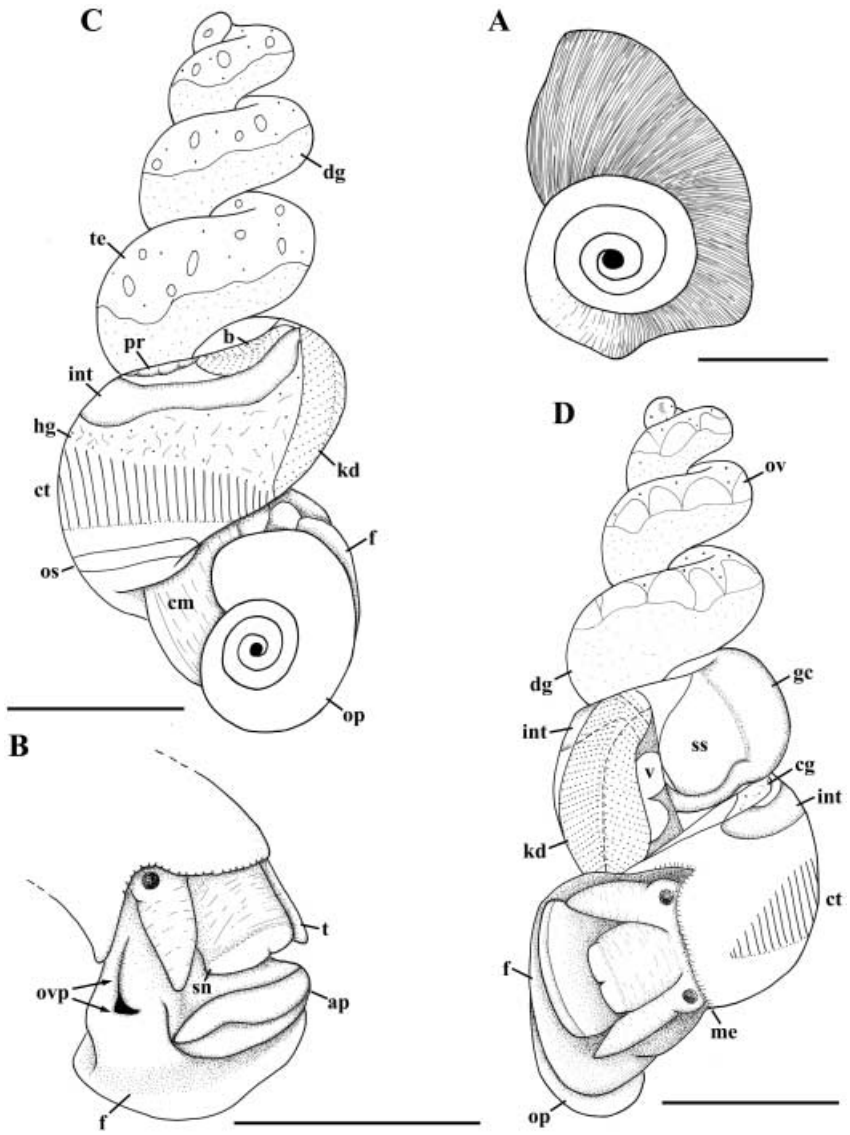

Fig. 14—External anatomy of *Martelia tanganyicensis* (ZMB 220067). —**A**. Operculum. Scale bar, 0.25 mm. —**B**. Ovipositor. External view of head–foot of female. Arrows indicate extent of pore aperture. —**C, D**. External anatomy. External view of male (C) and female (D) removed from shell. Dotted line in kidney roof (D) indicates extent of pericardium. Abbreviations: ap, anterior pedal gland; b, bladder; cg, capsule gland; cm, columellar muscle; ct, ctenidium; dg; digestive gland; f, foot sole; gc, gastric chamber of midgut; hg, hypobranchial gland; int, intestine; kd, main kidney chamber; me, mantle edge; op, operculum; os, osphradium; ov, ovary; ovp, ovipositor; pr, prostate; sn, snout; ss, style sac; t, cephalic tentacle; te, testes; v, ventricle. Scale bars, 0.5 mm, unless otherwise noted.

carina, forming nodes at intersection with axial elements. Axial elements gradually becoming more pronounced and decreasing in frequency.

Remarks. Apart from differences in thickness of shell and individual layers, shell microstructure (Fig. 13C) identical to *S. lacustris* and *A. giraudi*.

External anatomy. Operculum (Fig. 14A) comprising approximately four whorls. Propodium narrow but prominent, with pedal gland along anterior margin (Fig. 14B: ap). Metapodium reduced. Deep ovipositor pore (Fig. 14B: ovp) at base of short, thin groove on side of foot, below right eye and cephalic tentacle. Pore extending medially into foot, proximally with several folds of roughly equal size (Fig. 18A); dorsal fold rapidly becoming dominant with two opposing ventral folds forming Y-shaped lumen with surrounding basophilic subepithelial glands (Fig. 18B: se). At blind tip of pore, folds diminishing and lumen becoming irregular (Fig. 18C). Retracted cephalic tentacles short, thick, roughly equal to snout in length (Fig. 14B: t). Mantle cavity extending just under one whorl. Hypobranchial gland forming thick, warty pad in mantle roof. Dorsal and lateral mantle edge (Fig. 15A: me) evenly fringed. Ctenidium long, roughly one-half whorl in length, extending from near mantle edge to base of mantle cavity; axis of ctenidium straight (Fig. 15A: ct). Gill with ~17 leaflets (n = 2); leaflets triangular, asymmetric, with apices aligned on side opposite efferent branchial vessel. Osphradium (Fig. 15A: os) approximately one-half length of ctenidium, with pigmented axis and thin light-coloured rim; rim varying in thickness and sometimes becoming obsolete posteriorly adjacent to gill.

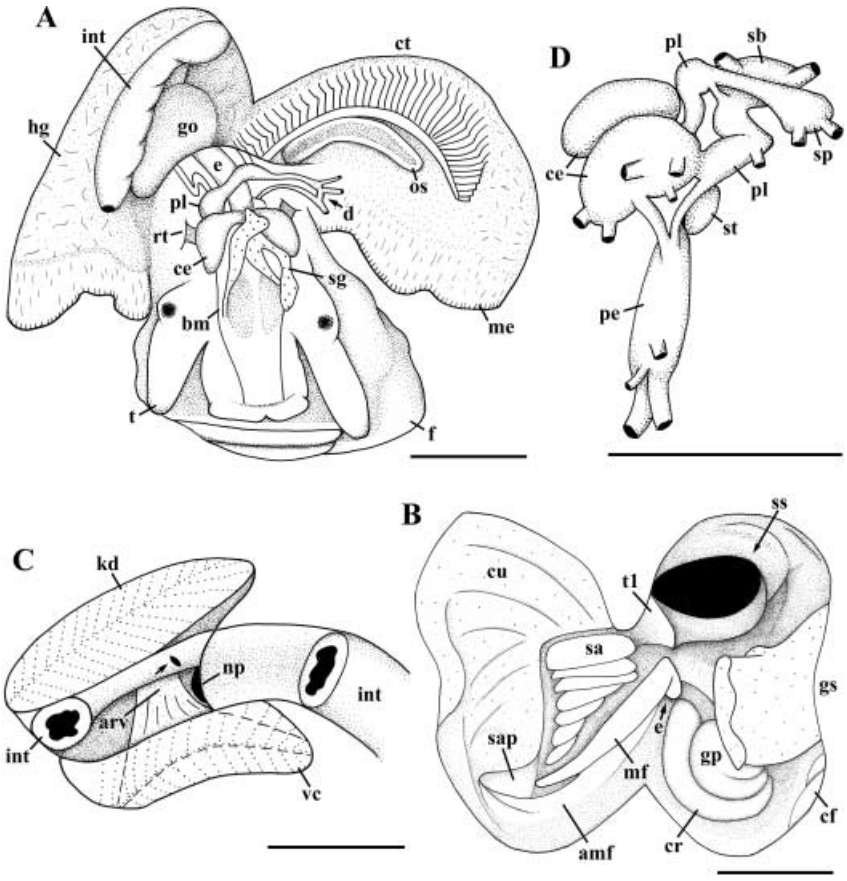

Fig. 15—External and internal anatomy of *Martelia tanganyicensis* (ZMB 220067). —**A**. Mantle cavity and cephalic haemocoele. Dorsal view, anterior is below. Stippling in buccal cavity indicates glandular epithelium alongside dorsal folds. —**B**. Midgut. Dorsal view, anterior is uppermost. —**C**. Kidney. Internal view of bladder. Lateral view, anterior is to the right. Segment of intestine excised and underlying kidney roof removed. Arrow indicates opening allowing communication between bladder and main kidney chamber. —**D**. Circumoesophageal nerve ring. Left lateral view, anterior is to the left. Abbreviations: amf accessory marginal fold; arv, afferent renal vessel; bm, buccal mass; ce, cerebral ganglion; cf, caecal fold; cr, crescentic ridge; ct, ctenidium; cu, cuticularized region of stomach roof; d, dialyneury; e, oesophagus; go, pallial gonoduct; gp, glandular pad; gs, gastric shield; hg, hypobranchial gland; int, intestine; kd, main kidney chamber; me, mantle edge; mf, marginal fold; np, nephropore; os, osphradium; pe, pedal ganglion; pl, pleural ganglion; rt, buccal mass retractor muscle; sa, sorting area; sap, sorting area pad; sb suboesophageal ganglion; sg, salivary gland; sp, supraoesophageal ganglion; ss, lip of style sac; st, statocyst; t, cephalic tentacle; t1, major typhlosole; vc, ventral kidney chamber. Scale bars, 0.25 mm.

Remarks. In comparison to the two preceding species, *M. tanganyicensis* is more similar to *S. lacustris* in overall dimensions and proportions of the soft body. However, the ovipositor shares features with both species; it is more similar to that of *A. giraudi* in external configuration, but is more similar to that of *S. lacustris* in the tripartite arrangement of folds in the interior, albeit briefly developed in the latter species. In general, the pattern of folds within the pore is unique in all three species, but typically results in the subdivision of the lumen such that bi-directional transport of fertilized eggs is possible. The ovipositor of *Martelia* is unique in the presence of subepithelial glands, in addition to the prismatic secretory cells lining the lumen of the pore. *Martelia* possesses a foot that is rather reduced compared to the others with an inconspicuous metapodium; this is evident histologically as well (Figs 6, 12 and 18) in the thickness and density of muscle fibres within the foot. The hypobranchial gland is not transversely grooved, but forms a thick pad in the mantle roof. The ctenidium is not markedly curved at the anterior end.

Alimentary system – Foregut. Radula (Fig. 16A–D) with 37 rows (n = 1 adult). Rachidian quadrangular, wider than tall, with prominent, central, sharply pointed cusp bounded by four to five pointed denticles on each side (Fig. 16B,C). Lateral teeth with short lateral extensions, roughly equal to cutting edge in length (Fig. 16A,B). Single, sharp prominent cusp flanked by approximately four inner and four outer pointed denticles. Denticles of rachidian and lateral teeth smooth, decreasing in size toward outer edges of tooth; denticle patterns variable within and between individuals.

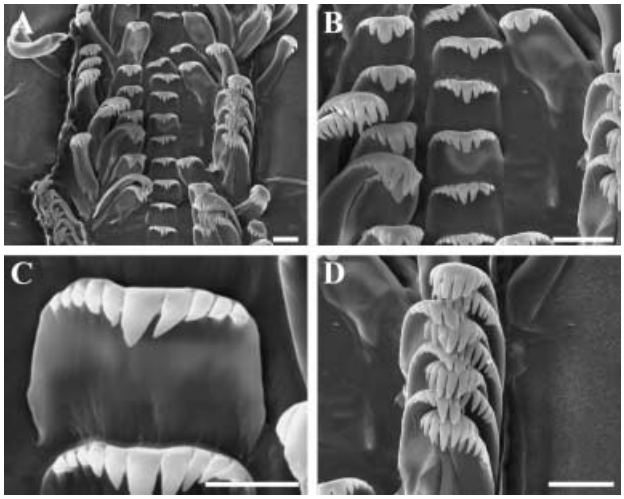

Fig. 16—Radula of *Martelia tanganyicensis* (ZMB 220067).
—**A**. View of entire width of ribbon. Scale bar, 10 μm.
—**B**. Detail rachidian and lateral teeth. Scale bar, 10 μm.
—**C**. Detail of rachidian cutting edge. Scale bar, 5 μm.
—**D**. Marginal teeth. Scale bar, 10 μm.

Marginal teeth with long, slender simple shafts and broadly rounded cutting edges. Inner and outer marginal teeth bearing slightly unequal numbers and sizes of denticles (Fig. 16D). Cutting edge of inner marginal tooth rather symmetric, bearing ~9–11 rounded denticles. Cutting edge of outer marginal bearing ~13 smooth, pointed denticles; denticles extending further down outer edge than inner edge.

Alimentary system – Midgut. Glandular pad (Fig. 15B: gp) short, rounded, barely extending past posterior end of gastric shield (Fig. 15B: gs). Posterior tip of accessory marginal fold (Fig. 15B: amf) curving slightly past posterior end of sorting area. Caecal folds paired.

Remarks. Overall, the radula is most similar to that of *S. lacustris* in size and shape of teeth and size and number of denticles, but is unique in the short lateral extensions and the slight asymmetry of the marginal teeth. Although considerably smaller than that of the other two species, the configuration of the foregut is shared between all three species. The midgut of *M. tanganyicensis* differs in the extent and curvature of the posterior end of the accessory marginal fold, the size of the sorting area and the number of sorting ridges. The configuration of caecal folds is more similar to *S. lacustris*, but the size and shape of the glandular pad is more similar to *A. giraudi*. Continuing the trend evident in *A. giraudi*, the recurvent segment of the hindgut of *M. tanganyicensis* is even shorter and follows a slightly curving course from the tip of the style sac to the right body wall under the kidney (Fig. 14D: int).

Reno-pericardial system. Horizontal subdivision of bladder lacking.

Remarks. Unlike the other two species, the kidney (Fig. 15C) lacks the horizontal subdivision of the bladder formed by sheets of excretory tissue extending from the front wall near the nephropore to the rear.

Nervous system. Buccal ganglia lying ventrolaterally on either side of radular sac. Cerebral ganglia (Fig. 15D: ce) each producing five nerves. Left pleural ganglion producing single pallial nerve. Each pedal ganglion producing two prominent anterior nerves and two smaller accessory nerves. Statocyst capsules bearing one slightly larger and several (roughly two to four) smaller statoconia.

Remarks. The nervous system differs from those of *S. lacustris* and *A. giraudi* in that fewer nerves are produced by the cerebral (five vs. six) and pedal (four vs. five) ganglia, and in the number of statoconia (approximately three to five vs. numerous).

Reproductive system – Female. Pallial oviduct forming simple straight tube, rectangular in shape posteriorly, tapering anteriorly to pointed tip. Capsule (Fig. 17A,B: cg) and albumen glands (Fig. 17A,B: ag) each forming roughly one-half of pallial oviduct. Glandular tissue regularly segmented within medial lamina (Fig. 17A), irregularly segmented in lateral lamina (Fig. 17B). Short, narrow anterior aperture (Fig. 17A) opening to spermatophore bursa (Fig. 17A: spb); bursa slightly shorter than capsule gland in length. Within bursa, short aperture (Fig. 17A) opening to capsule gland. Aperture bounded dorsally within medial lamina by shallow fold; fold continuing posteriorly over ventral channel (Fig. 17A: vc), eventually separating tiny, empty, blind pouch alongside spermatophore bursa. Ventral channel continuing posteriorly to short, blind extension functioning as seminal receptacle (Fig. 17A: rcs).

Reproductive system – Male. Prostate forming thick, glandular tube (Fig. 17C,D: pr), communicating with mantle cavity through slit-like anterior aperture (Fig. 17C). Prostate communicating laterally to elongate, tubular spermatophore-forming organ (Fig. 17C,D: sfo). Glandular tissue of lateral and medial laminae irregularly transversely segmented along entire length.

Remarks. The oviduct of *M. tanganyicensis* is most similar to that of *A. giraudi* with regard to the size of the spermatophore bursa and short communication between the bursa and gonoductal groove. *Martelia tanganyicensis* differs from both the preceding species in the minimal development of the dorsal fold and in the fact that it separates a small, non-functional pouch that functions as the seminal receptacle in the other two species.

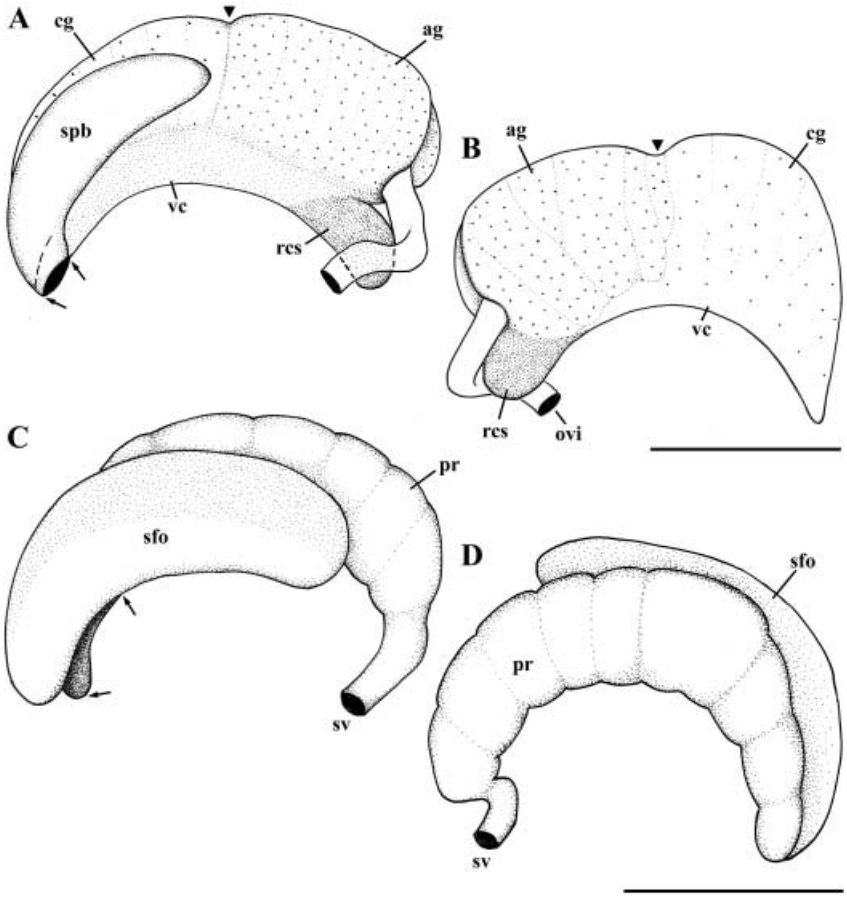

Fig. 17—Reproductive anatomy of *Martelia tanganyicensis* (ZMB 220067). —**A**. External, left lateral view of pallial oviduct. Anterior is to the left. Arrows indicate extent of opening between mantle cavity and spermatophore bursa; arrowheads indicate transition between albumen and capsule glands. Dotted line indicates communication between spermatophore bursa and gonoductal groove. —**B**. External, right lateral view of pallial oviduct. Anterior is to the right. —**C**. External, left lateral view of prostate. Anterior is to the left. Arrows indicate extent of opening between mantle cavity and gonoductal groove. —**D**. External, right lateral view of prostate. Anterior is to the right. Abbreviations: ag, albumen gland; cg, capsule gland; ovi, oviduct; pr, prostate; rcs, seminal receptacle; sfo, spermatophore-forming organ; spb spermatophore bursa; sv, seminal vesicle; vc, ventral channel. Scale bars, 0.25 mm.

The spermatophore organ differs from both *A. giraudi* and *S. lacustris* in size and left lateral position. In general, however, the size of the gonoduct aperture and overall size and shape of the spermatophore organ are most similar to *A. giraudi*.

Discussion

The present description is generally consistent with those of Mandahl-Barth (1954) and Bouillon (1955) to the extent that details were provided. One notable exception is the number of flanking denticles on the rachidian and lateral teeth, which were underestimated in both accounts; however, this may be a consequence of intraspecific variation, and/or reflects the technological limitations of the time. Additionally, Mandahl-Barth (1954) stated that there is no difference in the genital organs between *Syrnolopsis* and *Anceya*, which was found to be erroneous here. Bouillon (1955) indicated that the statocysts contain numerous statoconia, the jaw is more developed, the stomach more muscular, and the nervous system more condensed in *Martelia* as compared to the other two genera; however, these were not found in the present study.

Structural simplification and small body size

Syrnolopsines are noteworthy from the point of view that they are among the smallest species in the lake – *S. lacustris* and *A. giraudi* rarely exceed 10 mm in height, while *M. tanganyicensis* is typically smaller than 4 mm (see details, above). Other Lake Tanganyika gastropods that fall within this size range (less than ~8 mm in height on average) include *Stormsia minima* (Smith 1908) (2.58 ± 0.37 mm; $n = 100$), *Stanleya neritinoides* (Smith 1880) (5.32 ± 1.37 mm; $n = 178$), *Bathanalia straeleni* Leloup, 1953 (6.27 ± 3.36 mm; $n = 22$), *Mysorelloides multisulcata* (Bourguignat 1888) (6.45 ± 0.62 mm; $n = 9$) and species in the taxonomically complex genus *Bridouxia* Bourguignat, 1885 (e.g. *Bridouxia tanganyicensis* (Smith 1889) (2.93 ± 0.39 mm; $n = 66$). Syrnolopsines also represent the only lake clade, and higher taxonomic grouping, comprised exclusively of minute gastropods. According to the molecular phylogeny of Wilson *et al.* (2004), syrnolopsines represent an independent origin of small size from *Bridouxia* and *Stormsia*; the relationships of *Stanleya*, *Bathanalia* and *Mysorelloides* are currently unknown (see Fig. 19, and Affinities below).

Along the broad evolutionary continuum of size reduction, Hanken and Wake (1993) consider true miniaturization as

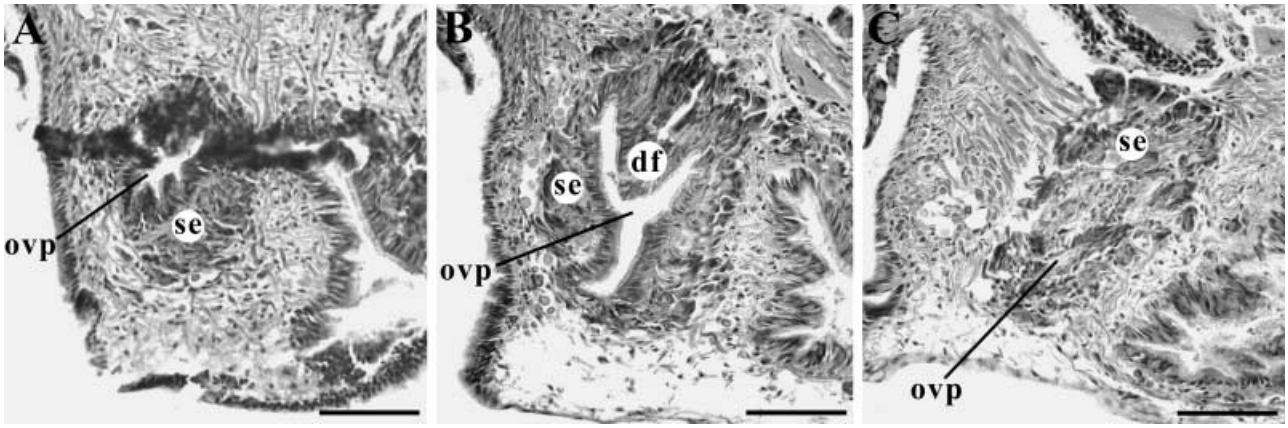

Fig. 18—Histology of the ovipositor of *Martelia tanganyicensis* (ZMB 220067). —**A**. Proximal pore with several fine folds. —**B**. Mid-pore with three opposing folds and Y-shaped lumen. —**C**. Inner pore with simple, irregular lumen. Abbreviations: ovp, lumen of ovipositor pore; df, dorsal fold; se, basophilic subepithelial glands. Scale bars, 50 μm.

the critical size at which important physiological or ecological functions (e.g. feeding, locomotion, reproductive biology) are affected. In light of the foregoing anatomical descriptions, syrnolopsines do not satisfy these criteria, even for the smallest – *M. tanganyicensis*. While some morphological features are somewhat simplified, all organs and organ systems are present and readily comparable in structure and organization to those of its larger sister taxa. However, size reduction often involves simplification of structures such that diagnostic features may become so modified that systematic affinities are unclear. A separate, but related issue, is that size reduction can often result in homoplasy so that unrelated miniaturized taxa are incorrectly considered to be monophyletic (e.g. Mooi 1990; Hanken and Wake 1993). Within this context, it is valuable to examine syrnolopsine anatomy to determine which features may be modified as a consequence of their small size, and so to explore the impact of small body size on putative homology assessment.

Comparison of these three species reveals several structural modifications/simplifications, particularly for *M. tanganyicensis*, that may be the consequence of size reduction. For example, the foot of *M. tanganyicensis* has become much reduced. Despite no obvious trend in length of the mantle cavity, the number of ctenidial leaflets decreases with size from *S. lacustris* with the highest number of leaflets (~80) to *M. tanganyicensis* with the lowest (~17 leaflets). The radula is approximately the same width in *S. lacustris* and *A. giraudi* (just over ~900 μm) (Figs 4 and 10), while it is a little more than half as wide in *M. tanganyicensis* (~550 μm) (Fig. 16). This decrease has been achieved not only through reduction in size of the teeth, but through loss of the long lateral extensions. It is interesting to note the allometric scaling of the foregut with respect to overall size; while adults of *M. tanganyicensis* are less than half the size of those of *S. lacustris*, the foregut occupies proportionately more volume in the cephalic haemocoele within the former (Figs 3A and 15A). The foregut is characterized by the presence of extremely short salivary gland ducts. In the midgut, the crescentic ridge is essentially L-shaped, and there is no caecum – a small pocket extending under the glandular pad behind the gastric shield. In *M. tanganyicensis*, the size of the sorting area and number of parallel ridges are reduced. In general, the intestine becomes shorter with decreasing species size – a common phenomenon among animals (see e.g. Rensch 1948). The statocysts bear only a few statoconia in *M. tanganyicensis* and the kidney has lost the horizontal sheet of excretory tissue within the bladder. For a summary of these and other morphological differences among syrnolopsines, see Table 1.

Hypotheses of causality concerning size reduction and corresponding changes in morphology are difficult to test, but one way to explore such issues is to assess parallel trends in other taxa that have become similarly reduced in size. Comparison with other lake species reveals that no single feature is universally shared among all small species listed above. However, several features are shared among the smallest thus far investigated – *M. tanganyicensis*, *Bridouxia tanganyicensis* and *S. minima*; these include reductions in the number of gill leaflets, sorting area ridges, intestine length, statoconia and allometric scaling of the foregut (Strong, unpublished data).

While size reduction has produced similar effects, it has not yielded identical results; in essence, differences in detail often make it possible to differentiate among these modifications. For example, although similarly reduced in the number of sorting ridges, the midgut of *Bridouxia* and *Stormsia* shares a number of unique features with their larger relatives (*Spekia*, *Reymondia*) (narrowly triangular sorting area, elongate glandular pad, linear crescentic ridge) that differentiate them from that of syrnolopsines (Strong, unpublished data). Reduction of the horizontal septum in the bladder from the large, flap-like condition in large lake

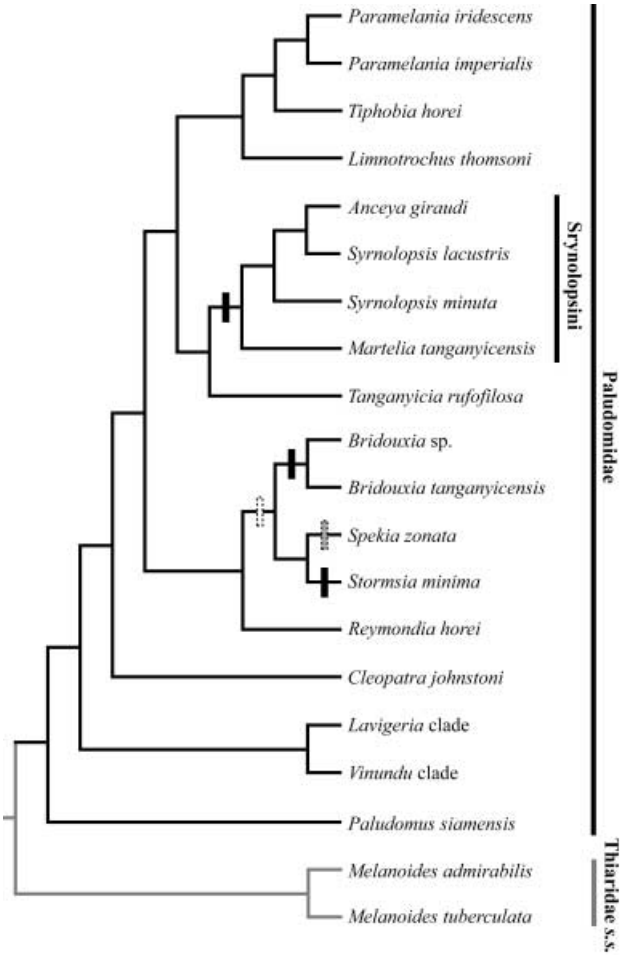

Fig. 19—Evolution of small adult body size mapped onto the cladogram based on combined 16S and COI sequences, adapted from Wilson *et al.* (2004: fig. 1). Black hash marks indicate the independent origin of small size in syrnolopsines, *Bridouxia* and *Stormsia*. Note that optimization of size is ambiguous as indicated by dotted hash marks; white indicates origin of small size, grey indicates reversal to large size in *Spekia zonata*. Other small taxa (*Stanleya neritinoides*, *Bathanalia straeleni*, *Mysorelloides multisulcata*) were not included and their phylogenetic affinities remain uncertain.

taxa is also not identical and can comprise a small but distinct ridge (*Bridouxia*, *Stormsia*) or can be completely absent (*M. tanganyicensis*). The number of statoconia is reduced in *Bridouxia* and *Stormsia*, but rather than a few statoconia of more or less equal size, they possess a single large statolith with several smaller statoconia. Thus, careful comparison of *Martelia* to *Bridouxia* and *Stormsia* reveals dissimilarities in detail that allow more rigorous putative homology assessment and are consistent with the interpretation that they have been independently derived (see Fig. 19).

Other anatomical modifications in syrnolopsines occur sporadically among some but not all small species (L-shaped crescentic ridge in the midgut) and occasionally occur in some large species as well (short lateral extensions on lateral teeth, short salivary glands, midgut caecum lacking) (Strong and Glaubrecht 2002, 2003, 2007). The taxonomic distribution of these characters and character states does not necessarily falsify the hypothesis that these features evolved as a consequence of reduction in size. Other lineage-specific factors (life habit, life history traits) probably influence and/or constrain the capacity for structures to respond to body size decreases. Additionally, retention of features in large descendants from a small 'ancestor' through heterochrony could explain such a pattern. While it is intriguing to speculate about the influence of size reduction on anatomy, such hypotheses must be further explored in the future within a phylogenetic framework incorporating all morphological characters.

Affinities of the Syrnolopsini

As stated above, based on their superficial conchological similarity to a variety of unrelated marine, freshwater and terrestrial families, the systematics of syrnolopsines has been highly unstable. Long after most other thalassoid gastropods were united and recognized as having cerithioid or 'thiarid' affinities, syrnolopsines remained in an isolated position or were allied to other superfamilies (e.g. Thiele 1929; Wenz 1939; Taylor and Sohl 1962). Consequently, the primary goal of the accounts of Mandahl-Barth (1954) and Bouillon (1955) was to establish their higher order placement and confirmed the basic cerithioid organization of the major organ systems; presence of a weakly paucispiral operculum, general shape and cusp patterns of the radular teeth, organization of the mantle cavity (smooth mantle edge, long monopectinate ctenidium, short osphradium), reproductive system (oviparous, presence of a seminal receptacle and nidamental gland in females and seminal vesicle in males, absence of a penis), and nervous system (condensed nerve ring, statocysts with numerous statoconia, lacking accessory pedal ganglia). Even after publication of these studies, however, the close relationship of syrnolopsines to other lake taxa was not consistently recognized (e.g. Brown 1980).

Today we have a much better understanding of the anatomy and systematics of the Lake Tanganyika thalassoid gastropods, specifically that they share unique features with the African genus *Cleopatra* and the Asian *Paludomus* that set them apart from the heterogeneous 'Thiaridae' (see e.g. Glaubrecht 1996; Strong and Glaubrecht 2002, 2003) to which family all these taxa have long been ascribed (see e.g. Boss 1978; Brown 1994; Michel 2004). Yet, in recent molecular analyses of Lake Tanganyika gastropods, the position of syrnolopsines is unstable. In two analyses based on partial cytochrome oxidase I (COI) sequences with *Anceya* as the only syrnolopsine representative, the tribe falls to the base of the ingroup in an unresolved polytomy (Michel 2004) or is united with *Paramelania* (West and

Table 1 Summary of major morphological differences within the Syrnolopsini

	Syrnolopsis lacustris	*Anceya giraudi*	*Martelia tanganyicensis*
External anatomy:			
Foot			Reduced
Ctenidial leaflets	79–80	59–60	17
Ovipositor groove	Absent	Present	Present
Ovipositor pore	U-shaped	H-shaped	Y-shaped; subepithelial glands
Alimentary system:			
Rachidian tooth	5/1/5	13–16/1/13–16	4–5/1/4–5
Lateral teeth	3–4/1/4–6	10–12/1/15–18	4/1/4
Lateral extensions	Moderate length	Moderate length	Short
Marginal teeth	13/13	Many/many	9–11/13
Recurvent segment of proximal intestine	Around distal one third of style sac	Around distal tip of style sac	Slightly curving
Reno-pericardial system:			
Bladder subdivided	Present	Present	Absent
Nervous system:			
Cerebral nerves	~6	~6	~5
Pedal nerves	~5	~5	~4
Statoconia	Many	Many	~3–5
Reproductive system:			
Opening between mantle cavity and bursa	Short	Long	Short
Opening between bursa and capsule gland	Long	Short	Short
Spermatophore bursa	Long	Short	Short
Seminal receptacle	Lateral	Lateral	Ventral channel
Opening between mantle cavity and prostate	Short	Long	Long
Spermatophore-forming organ	Pouch-like	Elongate	Elongate

Formula for radular tooth descriptions is as follows: (1) rachidian: number of denticles on left side/median cusp/number of denticles on right side, (2) lateral teeth: inner denticles/pronounced cusp/outer denticles, (3) marginal teeth: number of denticles on inner marginal tooth/number of denticles on outer marginal tooth.

Michel 2000). The analysis of Wilson *et al.* (2004), based on partial COI and 16S ribosomal DNA sequences, included multiple representatives of four syrnolopsine species (*S. lacustris*, *S. minuta*, *A. giraudi*, *M. tanganyicensis*) and supported a monophyletic Syrnolopsini as sister to *Tanganyicia rufofilosa* (Fig. 19). Thus, there is no consensus on their higher taxonomic placement, nor on their sister group relationships.

Despite modifications because of their small size, particularly in *Martelia* (see above), as well as several highly modified characters that distinguish them from all other lake species, syrnolopsines retain one important diagnostic feature – the presence of the spermatophore-forming organ. Thus, although studies continue to reveal high levels of morphological diversity and relatively few shared apomorphies among all Lake Tanganyika cerithioids, evidence continues to support the fact that thalassoid gastropods are united with *Cleopatra* and *Paludomus* in the Paludomidae and are distinguished from species formerly united in the Thiaridae *sensu lato*, most notably by the uniquely derived spermatophore-forming organ (see also Strong and Glaubrecht 2003: 263). Monophyly of the syrnolopsine assemblage, as indicated in the phylogeny of Wilson *et al.* (2004) (Fig. 19), is supported by the exceptional presence of salivary gland ducts that bypass the nerve ring and the linear albumen gland.

Based on what is known about the morphology of other lake species, is it possible to support their putative sister group placement to either *Paramelania* or *Tanganyicia* suggested by molecular studies? Mandahl-Barth (1954) indicated that the radula of *Tanganyicia* is very similar to that of *Syrnolopsis* and *Anceya*, in particular with regards to the shape and denticle patterns on the lateral and marginal teeth. However, this evidence is inconclusive because the range of variation in lateral and marginal cusp patterns among syrnolopsines overlaps with a number of taxa (e.g. *Limnotrochus*, *Paramelania*, *Bridouxia*, *Stormsia*) and the rachidian is more similar to that of *Limnotrochus* and *Paramelania* than to *Tanganyicia* (Leloup 1953; Strong and Glaubrecht 2002; and unpublished data).

More importantly, several key anatomical features set syrnolopsines apart from both *Paramelania* and *Tanganyicia*. In particular, the latter two possess a concentric operculum with a paucispiral nucleus, long salivary glands, a large U-shaped crescentic ridge within the midgut and a dialyneurous connection between nerves on the right side of the nerve ring. In this respect, syrnolopsines are more similar to *Stanleya*, which possesses a similar operculum (weakly paucispiral to multispiral), short salivary glands, similar midgut configuration and a condensed nerve ring with a zygoneurous connection on the right. From the point of view of overall similarity, a sister group relationship with *Tanganyicia*

Table 2 Summary of morphological differences between Syrnolopsini compared to select other Paludomidae

	Syrnolopsini	*Paramelania crassigranulata*	*Stanleya neritinoides*	*Tanganyicia rufofilosa*
External anatomy:				
Operculum	Weakly paucispiral	Concentric with paucispiral nucleus	Concentric with paucispiral nucleus	Multispiral
Alimentary system:				
Rachidian	Broadly rectangular	Broadly rectangular	Elongately rectangular	Elongately rectangular
Rachidian cusps	4–16/1/4–16	5–7/1/5–7	4–5/1/4–5	2–3/1/2–3
Lateral extensions	Moderately long/short	Long	Moderately long	Long
Salivary glands	Short	Long	Short	Long
Salivary gland position	By-pass NR	Pass through NR	Pass through NR	Pass through NR
Crescentic ridge	L-shaped	U-shaped	L-shaped	U-shaped
Accessory pad	Absent	Present	Present	Present
Caecal folds	Two	One	One	One
Caecum	Absent	Present	Present	Present
Nervous system:				
Dialyneury/zygoneury	Zygoneury	Dialyneury	Zygoneury	Dialyneury
Reproductive system:				
Pallial oviduct aperture	Small	~Anterior one-third to one-half	~Anterior one-half	~Anterior one-half
Albumen gland	Linear	Coiled	Coiled	Coiled
Seminal receptacle	Ventral channel/medial lamina	Ventral channel	Albumen gland	Ventral channel

Details from Strong and Glaubrecht (2002, 2003), unpublished data. Formula for rachidian tooth description follows Table 1. NR = circumoesophageal nerve ring.

or *Paramelania* does not seem likely (see Table 2). Assessing which of these features are plesiomorphies, synapomorphies, homoplasies or autapomorphies awaits a robust phylogenetic framework including all available morphological and molecular data.

Acknowledgements

We are indebted to Marilyn Schotte (USNM) for inking the anatomical drawings. E.S. is grateful to Marta deMaintenon (UH Hilo) for discussions on the evolution of small body size and its consequences. This study was funded by a grant of the Deutsche Forschungsgemeinschaft to M.G. (GL 297/5-1).

References

Ancey, C.-F. 1882. Les coquilles du lac Tanganyika. – *le Naturaliste* **4**: 38–39.

Bandel, K. 1998. Evolutionary history of East African fresh water gastropods interpreted from the fauna of Lake Tanganyika and Lake Malawi. – *Zentralblatt für Geologie und Paläontologie, Teil I* **1/2**: 233–292.

Boss, K. J. 1978. On the evolution of gastropods in ancient lakes. In Fretter, V. and Peake, J. (Eds): *Pulmonates, vol. 2a. Systematics, Evolution and Ecology*, pp. 385–428. Academic Press, London.

Bouchet, P. and Rocroi, J.-P. 2005. Classification and nomenclature of gastropod families. – *Malacologia* **47**: 1–397.

Bouillon, J. 1955. Sur l'anatomie et la position systématique du gastéropode thalassoide *Martelia tanganyicensis* Dautzenberg, 1908. – *Revue de Zoologie et Botanique Africaines* **52**: 233–240.

Bourguignat, J. R. 1885. *Notice Prodromique sur les Mollusques Terrestres et Fluviatiles Recueillis par M. Victor Giraud Dans la Région Méridionale du lac Tanganika*. Paris: Tremblay.

Bourguignat, J. R. 1888. *Iconographie Malacologiques Des Animaux Mollusques Fluviatiles Du Lac Tanganika*. Tremblay, Paris.

Bourguignat, J. R. 1889. *Mollusques de l'Afrique équatoriale de Mogue-douchou à Bagamoyo et de Bagamoyo au Tanganika*. D. Dumoulin, Paris.

Bourguignat, J. R. 1890. Histoire malacologique du lac Tanganika (Afrique équatoriale). – *Annales Des Sciences Naturelles de Paris, Zoologie* **10**: 1–267.

Brown, D. S. 1980. *Freshwater Snails of Africa and Their Medical Importance*, 1st edn. Taylor & Francis, London.

Brown, D. S. 1994. *Freshwater Snails of Africa and Their Medical Importance*, revised, 2nd edn. Taylor & Francis, London.

Coulter, G. W. (Ed.) 1991. *Lake Tanganyika and its Life*. Oxford University Press, London.

Crosse, H. 1881. Faune malacologique du Lac Tanganyika. – *Journal de Conchyliologie* **29**: 105–139.

Dartevelle, E. and Schwetz, J. 1948. Le Lac Tanganika. – *Mémoires du Institut Royal Colonial Belge* **14**: 1–118.

Fischer, P. 1887. *Manuel de Conchyliologie et de Paléontologie Conchyliologique; ou, Histoire Naturelle des Mollusques Vivants et Fossiles*. Librairie F. Savy, Paris.

Germain, L. 1908. Mollusques du Lac Tanganyika et de ses environs. Résultats Scientifiques des Voyages en Afrique d'Édouard Foà. – *Bulletin du Muséum d'Histoire Naturelle* **14**: 1–612.

Glaubrecht, M. 1996. *Evolutionsökologie und Systematik Am Beispiel Von Süß- und Brackwasserschnecken (Mollusca: Caenogastropoda: Cerithioidea): Ontogenese-Strategien, Paläontologische Befunde und Historische Zoogeographie*. Backhuys Publishers, Leiden.

Glaubrecht, M. and Strong, E. E. 2004. Spermatophores of thalassoid gastropods (Paludomidae) in Lake Tanganyika, East Africa, with a survey of their occurrence in Cerithioidea: functional and phylogenetic implications. – *Invertebrate Biology* **123**: 218–236.

Gorthner, A. and Meier-Brook, C. 1985. The Steinheim basin as a paleo-ancient lake. In Bayer, U and Seilacher, A. (Eds): *Sedimentary and Evolutionary Cycles*, pp. 211–223. Springer Verlag, Berlin/Heidelberg/New York/Tokyo.

Hanken, J. and Wake, D. B. 1993. Miniaturization of body size: organismal consequences and evolutionary significance. – *Annual Review of Ecology and Systematics* **24**: 501–519.

Houbrick, R. S. 1988. Cerithioidean phylogeny. – *Malacological Review, supplement* **4**: 88–128.

Humason, G. L. 1967. *Animal Tissue Techniques*. W.H. Freeman, San Francisco.

Leloup, E. 1953. *Exploration hydrobiologique du Lac Tanganika (1946–47)*, Vol.3, Fascicule 4, Gastéropodes. Institut Royal des Sciences Naturelles de Belgique, Brussels.

Mandahl-Barth, G. 1954. The anatomy and systematic position of the Tanganyika snails *Syrnolopsis* and *Anceya*. – *Annales du Musée Royal de L'afrique Centrale, Sciences Zoologiques, Tervuren, Belgium* **1**: 217–221.

Martens, K. 1997. Speciation in ancient lakes. – *Trends in Ecology and Evolution* **12**: 177–182.

Michel, E. 2004. *Vinundu*, a new genus of gastropod (Cerithioidea: 'Thiaridae') with two species from Lake Tanganyika, East Africa, and its molecular phylogenetic relationships. – *Journal of Molluscan Studies* **70**: 1–19.

Mooi, R. 1990. Progenetic miniaturization in the sand dollar *Sinaechinocyamus*: implications for clypeasteroid phylogeny. In de Ridder, C., Dubois, P., Lahaye, M. C. and Jangoux, M. (Eds): *Echinoderm Research. Proceedings of the Second European Conference on Echinoderms, Brussels, 18–21 September 1989*, pp. 137–143. AA. Balkema, Rotterdam and Brookfield.

Moore, J. E. S. 1899. On the hypothesis that Lake Tanganyika represents an old Jurassic Sea. – *Quarterly Journal of Microscopical Science* **41**: 303–321.

Moore, J. E. S. 1903. *The Tanganyika Problem*. Hust and Blackett, London.

Pilsbry, H. A. and Bequaert, J. 1927. The aquatic mollusks of the Belgian Congo. With a geographical and ecological account of Congo malacology. – *Bulletin American Museum of Natural History* **53**: 69–602.

Rensch, B. 1948. Histological changes correlated with evolutionary changes of body size. – *Evolution* **2**: 218–230.

Smith, E. A. 1880. On the shells of Lake Tanganyika and of the neighbourhood of Ujiji, Central Africa. – *Proceedings Zoological Society London* **1880**: 344–352.

Smith, E. A. 1881. On a collection of shells from Lakes Tanganyika and Nyassa and other localities in East Africa. – *Proceedings of the Zoological Society of London* **1881**: 276–300.

Smith, E. A. 1890. On a new genus and some new species of shells from Lake Tanganyika. – *Annals and Magazine of Natural History* **1890**: 93–96.

Strong, E. E. and Glaubrecht, M. 2002. Evidence for convergent evolution of brooding in a unique gastropod from Lake Tanganyika: anatomy and affinity of *Tanganyicia rufofilosa* (Smith, 1880) (Caenogastropoda, Cerithioidea, Paludomidae). – *Zoologica Scripta* **31**: 167–184.

Strong, E. E. and Glaubrecht, M. 2003. Anatomy and systematic affinity of *Stanleya neritinoides* (Smith, 1880), an enigmatic member of the thalassoid gastropod fauna from Lake Tanganyika, East Africa (Cerithioidea, Paludomidae). – *Acta Zoologica* **84**: 249–265.

Strong, E. E. and Glaubrecht, M. 2007. The morphology and independent origin of ovoviviparity in *Tiphobia* and *Lavigeria* (Caenogastropoda, Cerithioidea, Paludomidae) from Lake Tanganyika. – *Organisms, Diversity and Evolution* **7**: 81–105.

Taylor, D. W. and Sohl, N. F. 1962. An outline of gastropod classification. – *Malacologia* **1**: 7–32.

Thiele, J. 1929. *Handbuch der Systematischen Weichtierkunde*. Fischer, Jena.

Van Damme, D. and Pickford, M. 2003. The late Cenozoic Thiaridae (Mollusca, Gastropoda, Cerithioidea) of the Albertine Rift Valley (Uganda-Congo) and their bearing on the origin and evolution of the Tanganyikan thalassoid malacofauna. – *Hydrobiologia* **498**: 1–83.

Wenz, W. 1939. *Handbuch der Paläozoologie. Band 6. Gastropoda. Teil 3: Prosobranchia*. Gebrüder Borntraeger, Berlin.

West, K. and Cohen, A. 1994. Predator–prey coevolution as a model for the unusual morphologies of the crabs and gastropods of Lake Tanganyika. – *Advances in Limnology* **44**: 267–283.

West, K. and Cohen, A. 1996. Shell microstructure of gastropods from Lake Tanganyika, Africa: adaptation, convergent evolution and escalation. – *Evolution* **50**: 672–682.

West, K. and Michel, E. 2000. The dynamics of endemic diversification: molecular phylogeny suggests an explosive origin of the thiarid gastropods of Lake Tanganyika. – *Advances in Ecological Research* **31**: 331–354.

West, K., Cohen, A. and Baron, M. 1991. Morphology and behaviour of crabs and gastropods from Lake Tanganyika, Africa: implications for lacustrine predator–prey coevolution. – *Evolution* **45**: 589–607.

Wilson, A. B., Glaubrecht, M. and Meyer, A. 2004. Ancient lakes as evolutionary reservoirs: evidence from the thalassoid gastropods of Lake Tanganyika. – *Proceedings of the Royal Society of London, Biological Sciences* **1538**: 529–536.